Alma Mater Studiorum – Università di Bologna

DOTTORATO DI RICERCA IN

CHIMICA

Ciclo XXVIII

Settore Concorsuale di afferenza: 03/A1- CHIMICA ANALITICA

Settore Scientifico disciplinare: CHIM/01-CHIMICA ANALITICA

IMPLEMENTATION OF CHEMILUMINESCENCE AND COLOR-BASED DETECTION IN SMARTPHONE FOR BIOASSAYS.

Presentata da: Calabria Donato

Coordinatore Dottorato   **Relatore**

Chiar.mo Prof. Aldo Roda   **Prof. Aldo Roda**

Esame finale anno 2016

CHAPTER 1

Introduction

1.1 Introduction

There is a strong interest in the use of smartphone, alone or in conjunction with add-on devices as new generation POC diagnostic device. In recent years, the development of an accurate and user-friendly diagnostic device for point-of-care (POC) applications has received increasing attention in the field of analytical chemistry [1][2][3][4][5][6][7][8][9].

The POC systems   perform in-site tests providing fast and reliable analytical results, with the advantages of low sample and reagent consumption,   rapid and easy analysis, reduced costs, possibility of extra-laboratory application. Fulfill minimum requirements [10] that characterize a real POC system are:

- the direct introduction of the sample without or with few steps of purification and pretreatment of sample

- Reduced dimensions, be portable with a little weight and autonomous electrical power
- be easy to use, in order to be used by unskilled operators outside of standard equipped laboratories
- provides qualitative and quantitative results by analyzing and processing data outputs measured by portable device detector.

Moreover an ideal POC device should be fabricated with low cost and disposable elements, and at the same time, it should ensure stability and durability. Such analytical tool should be capable of automating the analysis (sample pre-treatment, reagents delivery, mixing, separation and detection) and determining multiple analytes (showing

multiplexing capability) and providing wide measurement range of analysis performances. Moreover point-of-care device should be robust and such as the tolerant to changes in air humidity and temperature [11].

The emerging field of analytical chemistry to develop portable miniaturized and self-operating system, in which is possible to scale down and transfer traditional bench-top analytical procedures, can pave the way for extra-laboratory analyses in clinical chemistry, environmental monitoring, food analysis, and bio-warfare protection [12]. A other characteristic of a good point of care device is the capability to use very small sample volumes, achieving low limits of detection of analyte of interest and the possibility to perform the test in shorten time and cost of analysis.

Smartphones, thanks to their multifunction capabilities, imaging, and computing power, and the possibility to extend built-in functions of smartphones, can be considered as the natural evolution of point-of-care (POC) analytical devices. Smartphones offer photography (still and video), location and other sensors (global positioning system [GPS], accelerometers, etc.), the long-distance transfer of information (data and images) via text messaging (Short Message Service – SMS), built-in apps (e-mail, calendar, document readers, etc.), and wireless data service. Moreover, hundreds of new applications (apps) are made available every day. The extensive distribution of smartphones and tablets, together with cloud services ensuring pervasive connectivity, creates an incredible market, largely untapped, especially in the field of healthcare self-management. So, smartphone itself can act as a transducer or detector and perform data analysis. The main advantage in comparison to existing biosensor diagnostic devices is the challenge to develop an user-friendly "all-in-one device" and the possibility to

perform analytical tests outside clinical laboratories by no-dedicated and unskilled equips. After running the analytical assay, it is possible to process data and sent results by E-mail, for example, to a physician for the diagnosis.

In literature, there are many examples of smartphone use as analytical device to perform diagnostic tests. Increasing interest in using smartphones to detect analytes of clinical interest [13] is due to the ubiquitous distribution and international connectivity of smartphones and, it is due to changing the concept of mobile health.

The exponentially increasing performance of CMOS-based photocameras, and the possibility to augment smartphone capabilities by other additional accessories make appropriate to use smartphone as portable biosensors and point-of-care platforms for healthcare, food safety, environmental monitoring, and biosecurity, especially in remote and rural areas.

The continuous improvement of smartphone electronics and the development of new apps have stimulated research to expand the applications of smartphone photocamera as a "smart detector" to develop new diagnostic and prognostic tests for a large number of pathologies and for evaluating pharmaceutical therapies, integrating several optical-based methods as absorbance, reflectance, fluorescence and SPR.

1.2 Classification of smartphone based biosensors

The classification of smartphone-based point-of-care devices is based on way of using smartphone technologies. It is possible distinguish two main categories: smartphone used as detector and smartphone used as instrumental interface.

1.2.1 Smartphone as detector.

In literature there are many examples of biosensors based on the integration of smartphone technology in complementary-coupled accessories as cartridges and other components needed to perform analytical tests. The smartphone chamber is used to detect the output signal. Breslauer et al., have reported the development of smartphone-based microscope for both bright-field and fluorescence imaging [14]. The apparatus of the device is composed by a standard microscope eyepiece, an emission filter, an objective, a condenser lens, an excitation filter, a collector lens, and an LED as excitation source (Figure 1.1). The filters and LED can be removed to transform the system in a bright-field microscope. The device, thanks to the camera's high resolution, is able to image blood cell and microorganism morphology and it has been applied for clinical diagnostics by capturing bright-field high-resolution images of *P. falciparum* malaria-infected blood samples and fluorescent images of Auramine-O-stained *M.-tuberculosis*-positive sputum smears.

Another example where the smartphone's camera is used as a microscope, has been reported by Tseng et al. The system is very simple and elementary of the previous. The device does not provide for the using of lenses, laser, or other optical components, greatly

simplifying the system architecture [15]. It consists only of a LED to vertically illuminate the sample area. The LED light, that interacts with the sample, is scattered and refracted. The light waves that pass through the sampled objects (e.g. cells) interfere with the unscattered light, creating a hologram of each object, which is detected using the smartphone camera (Figure 1.2). The device is able to image various sized microparticles, red and white blood cells, platelets, and parasites. This lens-free smartphone microscope has several important features, including compactness, lightness (38 g), and cost-effectiveness, which make it very suitable for decentralized point-of-need use, particularly in developing areas.

The problems associated with this kind of applications of the smartphone's camera, are connected to the image spatial resolution, limited by the pixel size at the sensor, making the system less accurate than a standard microscope. Moreover, the image process needed to obtain the holographic reconstruction must be performed remotely, e.g. in a central hospital, because it would drastically reduce the speed of smartphone computing.

The smartphone's camera has been also used as a detector for the development of a smartphone-based rapid-diagnostic-test (RDT) reader platform for LFIA [16], and for fluorescence measurements and photometry. Erickson et al. have reported a portable smartphone device based on reflectance photometry to quantify cholesterol levels in blood. The accessory connected to smartphone is composed of a cartridge, and a strip on which the color-based assay takes place [17]. The reaction area is illuminated by the built-in smartphone flash. Thanks to a dedicated app, the device correlates the variations of color and brightness to analyte concentrations.

Preechaburana et al. proposed for the first time, the integration of angle-resolved surface plasmon resonance (SPR) detection techniques in smartphone technology to detect and quantify β2 microglobulin (β2M) levels in serum and urine [18] (Figure 1.3). This analyte is a biomarker for cancer, inflammatory disorders, and kidney disease. Even if smartphone based-SPR device performance is related to the spatial resolution of the smartphone camera, its platform's resolution is comparable with compact conventional analytical SPR devices.

Finally, smartphone camera has been used as detector to develop a portable miniaturized spectrometer for a label-free photonic crystal biosensor [19]. The smartphone-based device needed of optical components (collimator, polarizer, photonic crystal, and grating), and of an app to process the camera images into the photonic crystal transmission spectrum (Figure 1.4). The device has been used to detect an immobilized protein monolayer and a concentration-dependent antibody binding to a functionalized photonic crystal. Moreover, the system is able to work only in a dry state.

1.2.2 Smartphone as instrumental interface

Alternatively, the smartphone can be used as instrumental interface, connecting the smartphone with the bioanalytical device for example via a micro-USB port, Bluetooth, or Wi-Fi. In this case, the smartphone isn't used as detector, but are exploited its computing capabilities to control the experimental setup and display the test results on the screen. In literature there are few examples of this approach, while some commercial applications are very interesting.

Stedtfeld et al. developed a portable device called Gene-Z to quantify and detect rapidly multiple genetic markers by parallel analysis. [20]. It consists of a microfluidic chip composed of four arrays of 15 reaction wells. Each well contains complementary dehydrated primers for isothermal amplification. This device is able to perform simultaneous analysis of four samples. The Gene-Z can be controlled by an iPod Touch, to compute and elaborate data and send the results of analysis via a Wi-Fi interface (Figure 1.5).

Among commercially available platforms connected with a smartphone, ethylometers and glucometers are essentially the most common examples. In particular, two main examples of smartphone based-breath sensors for detection of alchol are commercially presented by Europe company Vodafone (Floome) [21], and by US company, Breathometer Inc. [22]. Among smartphone-interfaced glucometer now commercially available, there are the glucometer iBGStar® (Sanofi) and two kinds of glucometer for smartphone developed by iHealth Lab Inc.: iHealth Align [23] and a wireless smart gluco-monitoring system [24]. iHealth Align is the world's smallest FDA-approved mobile glucometer, which plugs directly into the smartphone's audio jack. The device is controlled by an app that instantly displays results on the screen and automatically keeps a history of the data. The smart glucometer is wireless, portable, and connects to the smartphone or tablet using Bluetooth technology to give the test result in five seconds. It automatically records all glucose readings and tracks the quantity and expiration date of the test strips. Both the glucometers work with Apple devices and offer the option of sharing the information with a doctor or caregiver.

1.2.3 Electrochemical detection

A very useful way to use your smartphone as instrumental interface can be exploited by its integration with electrochemical detection methods. Lillehoj et al. developed an electrochemical detection method-based platform connected via mini-USB port to smartphone. [25]. The device is composed of an embedded circuit for signal processing and data analysis, and of a disposable microfluidic chip for fluidic handling and biosensing (Figure 1.6). This system has been used to detect the malaria biomarker *Plasmodium falciparum* histidine-rich protein 2. The LOD is of 16 ng/mL in human serum, which is a value comparable with standard instrumentation. The assay is perfomed in 15 min.

The main disadvantage of these systems is the need to integrate the smartphone with devices such as electrical circuits, electrodes, and potentiostats. This requires additional costs and a more complex system. Furthermore, these devices are often connected to the smartphone, increasing its energy consumption. A lower power microcontroller is then required to secure a more efficient power rectification.
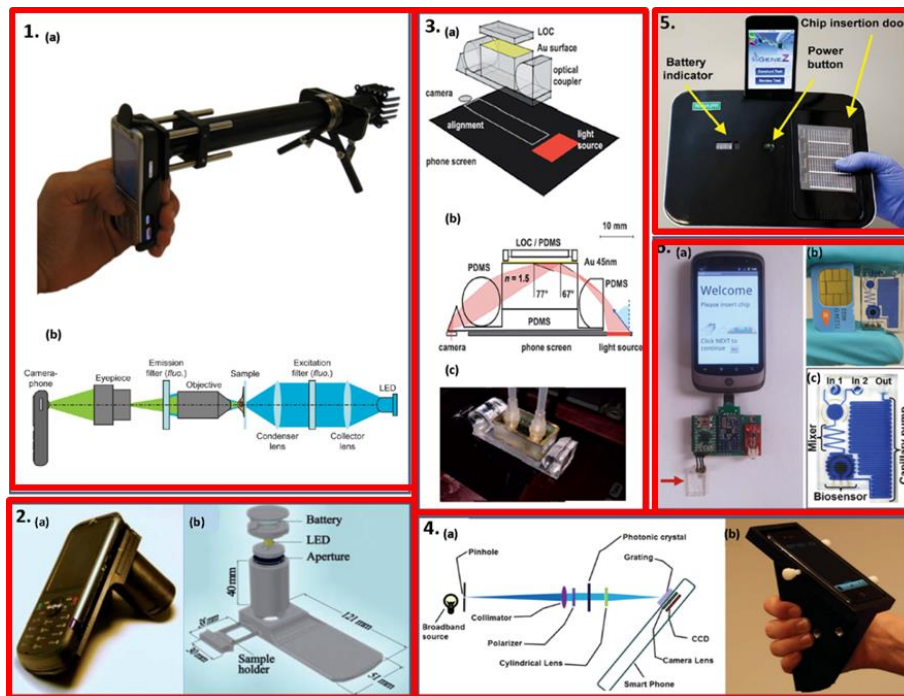
Figure 1. Panel 1: (a) a current prototype, with filters and LED installed, capable of fluorescence imaging and (b) cellphone microscopy optical layout for fluorescence and bright-field imaging (components required for fluorescence imaging only are indicated by 'fluo'). Panel 2: (a) lens-free cellphone microscope which operates based on incoherent in-line holography and (b) schematic diagram of the microscope attachment. Panel 3: (a) 3D scheme of a representative setup for angle-resolved SPR using screen illumination and front camera detection optically coupled with a disposable device, (b) 2D raytrace of the experimental arrangement showing the light path from screen to camera, and (c) picture of the actual experimental arrangement. Panel 4: (a) schematic of the optical components within the smartphone cradle and (b) photo of the cradle with a PC biosensor slide inserted into the detection slot. Panel 5: picture of the Gene-Z prototype with the iPod docked on the recharge port and the disposable chip sitting on the door that is used for insertion. Panel 6: (a) photograph of the assembled prototype device (the arrow indicates the microfluidic chip), (b) photograph of the chip and a cellphone SIM card for comparison and (c) an enlarged image of the chip with labeled components (the channels are filled with dye for improved visualization of the fluidic network).

The smartphone-based biosensor can be classified according to the analytical detection method used.

1.3 Smartphone-based biosensors

Several works have been reported in which different detection principles have been used to develop smartphone-based biosensors that do not need additional devices, and they perform the entire analytical process, from analysis to data acquisition and elaboration.

1.3.1 Color-based detection

The development of analytical point of care devices that exploit color change to detect analytes of interest has attracted much attention. Generally these systems are inexpensive, stable, simple to realize. Moreover, CMOS array of smartphone camera is able to respond to red, green and blue (RGB) light. Today, smartphones integrate several function dedicated to make better the acquisition of image such as the automated Auto White Balance (AWB), which allow to adjust the detected RGB signals at differents ratios, reproducing good colors [26]. The availability of an increasing number of mobile apps for photo editing, RGB color analysis, and image processing, make easier the quantitative analysis of the collected data. These biosensors are characterized by a relatively low sensitivity and can therefore be used to detect analytes present in relatively high concentrations in biological fluids and environmental and food samples.

1.3.2 Absorbance-based devices

These cellphone based-platforms are real miniaturized spectrophotometers. They have a complementary attachment, composed of an inexpensive plastic plano-convex lens, light-emitting

diodes (LEDs) to vertically illuminate the test and control cuvettes, specifically chosen to match the absorption spectrum of the colorimetric assay performed in the test tube with wavelength of LEDs, light diffusers, circular apertures to spatially control the imaging field-of-view, a digital test reader and a smart application that measures the absorption of colorimetric assays. The transmitted light through the sample and control cuvettes is imaged onto the digital camera of the smartphone using a plano-convex lens. The limitations of these sensors are based on the difficulty of use these devices by unskilled personnel and by the complexity of the various device accessories (which often necessitate changing the smartphone's physical and electronic components), the need to use laboratory instruments (such as pipettes) because reactions are performed in solution, the difficulty of storing reagents, and the incubation times.

An interesting application of this kind of point-of-care biosensors has been presented by Ozcan's research group. They developed a smartphone-based device for quantifying mercury (II) ions in water, using a plasmonic gold nanoparticle (AuNPs) and aptamer colorimetric transmission assay [27]. The chemical assay principle is based on different affinity of Thymine-rich sequence aptamers (5'-TTTTTTTTTT-3') toward gold nanoparticles and toward mercury ions and on the effect of absorption due to the degree of aggregation of gold nanoparticles. In the absence of mercury, the aptamer covers the surface of the gold nanoparticles and prevents the aggregation. In presence of mercury (II) ions, aptamers form a more stable complex T-Hg^{2+}-T. To quantify mercury ion concentration (LOD ~ 3.5 ppb) is used a two-color ratiometric detection method. The change of ratio between transmitted light at two wavelengths (523 nm, green and 625 nm, red) is thus related to AuNPs aggregation. The smartphone accessory is

composed of two battery-alimented LEDs emitting light at 523 nm (green) and 625 nm (red) to follow the shift in the extinction wavelengths of the dispersed and aggregated AuNPs, respectively; a light diffuser; a chamber for sample and control cuvettes; and an external lens to converge transmitted light and focus two color images.

Vashist et al. have recently reported a smartphone-based colorimetric reader to detect human C-reactive protein (CRP) by an immunoenzymatic assay. [28].

1.3.3 Reflectance-based devices

Other devices use light reflectance to measure an end-point enzymatic reaction. Enzymes specific to a given analyte are immobilized on test strips. The reflected light color intensity of a chromogenic substrate is directly related to the amount of analyte in the biological fluids.

The research group of Erickson has developed several systems that use dry reagent chemistry test based on light reflectance principle as detection method. They developed a smartphone-based device that uses uses dry reagent test strips manufactured by CardioChek (Polymer Technology Systems Inc., IN, USA) to quantify cholesterol levels in serum, called smartCARD (smartphone Cholesterol Application for Rapid Diagnostics) system [29]. The strip is composed of a series of filter papers that separate plasma from red blood cells and direct some of the plasma towards an analyte-specific reaction pad (Figure 2). The enzymatic conversion of cholesterol and HDL by the cholesterol oxidase with the production of hydrogen peroxide and next reaction between this latter and an appropriate dye, leads to a color change in the detection area related to the concentration of analyte. As

light source, the smartphone accessory exploits the built-in flash illumination technology. To ensure a uniform illumination for repeatable image acquisition of the test strip, the device is equipped with a black PDMS diffuser ensures uniform illumination. An app developed for the iPhone iOS platform analyzes color parameters such as hue, saturation, and luminosity from the acquired image of the test area, quantifying physiological total cholesterol levels in blood (100 – 400 mg/dL) within 60s by imaging the standard test strips.

Smartphone-based test reader platforms of different formats based on lateral flow immunochromatographic assays have been reported [30][31][32][33]. Various types of test strips can be integrated into the accessory device attached to the smartphone. Erickson's group developed one example of reflectance-based smartphone device for a LFIA assay (vitaAID) to evaluate vitamin D levels in serum. [34]. The analytical colorimetric detection principle to quantify 25-hydroxyvitamin D is a gold-nanoparticle-based immunoassay (Figure 2).

The advantages of using these systems are due to operative simplicity thanks to which even unskilled persons can perform the tests, to the low cost of material used to realize them and to the reduced sizes of the devices and to need of using few volumes of sample for analysis. Furthermore, the availability of several colorimetric tests, make possible the analysis of a wide range of analytes.
 However, there are also limitations. The results of analysis can be affected by variations in wetting time, environmental temperature, light, and humidity and homogeneity of light and color, that make difficult to obtain a quantitative information and to the possibility to quantify samples with high concentrations of analytes. (e.g. millimolar).
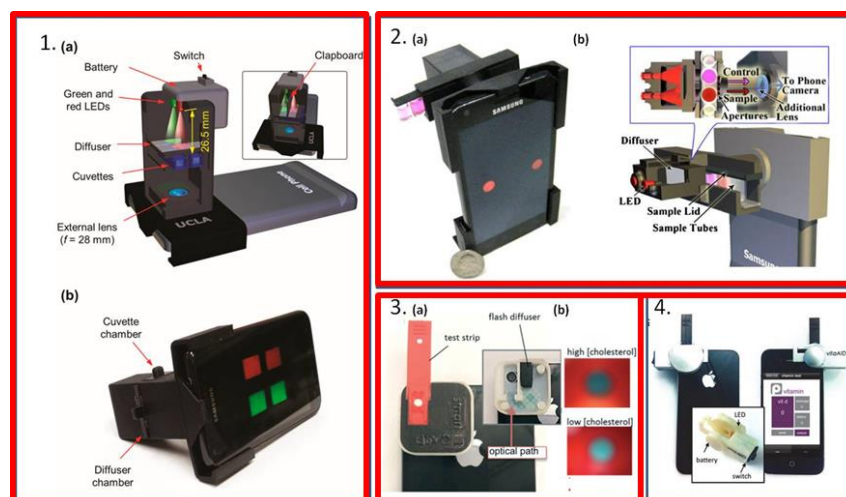
Figure 2. Panel 1: (a) 3D schematic illustration of the internal structure of the opto-mechanical attachment of the ratiometric optical reader on smartphone. (b) Photograph of screen of the smartphone displaying a typical image of the sample and control cuvettes when illuminated by red (625 nm) and green (523 nm) LEDs simultaneously. Panel 2: (a) Image of the iTube platform and smartphone screen of colorimetric assays reading. (b) A schematic illustration of components of the same iTube platform. Panel 3: a) Image of the smartCARD accessory and the test strip used; the inset shows the inside of the accessory with the black PDMS diffuser and the optical path of the flash used to illuminate the strip. b) Image of low cholesterol strip (<100 mg dl^{-1}) and high cholesterol (>400 mg dl^{-1}) strip camera acquisitions. Panel 4: Image of vitaAID accessory on a iPhone with the inset showing the components of the accessory.

1.3.4 Photoluminescence detection

Photoluminescence is another analytical method of detection that has been integrated with smartphone's camera. In this case the instrumentation is more complex because it includes an optical module comprising a light source, optical filter, and lens. The measurement cell must also meet specific geometrical and transparency requirements. Despite these limitations, fluorescence is widely used as a detection principle in smartphone-based biosensors thanks to its high sensitivity.

Rajendran et al. developed a smartphone-based fluorimeter to detect the foodborne bacterial pathogens, Salmonella and Escherichia coli O157, by a conventional LFIA assay. [35]. The fluorophore (FITC) is doped in silica nanoparticles (SiNPs) conjugated to the biospecific respective antibodies. The components of this fluorimeter are a lightweight optical module containing an LED light source, a fluorescence filter set, and a lens attached to the integrated smartphone camera, which acquired high-resolution fluorescence images.

Ozcan's group developed another portable smartphone-based device albumin tester to quantify albumin concentration in urine samples, using a sensitive and specific fluorescent assay performed in a disposable test tube [36]. Recently, has been presented a fluorescence sandwich immunoassay assay for prostate-specific antigen (PSA) [37]. The performances of smartphone's camera are enhanced with a magnifying lens. Other components are a simple light source, and a miniaturized immunoassay platform, the transparent Microcapillary Film (MCF).

1.4 Chemical Luminescence systems

Luminescence is a spontaneous emission of radiation following the decay of a species from an electronically excited state to its ground state. Among different types of luminescence, we can distinguish the chemical luminescence, which consists in the phenomenon of luminescence via chemical reaction. Depending on type of stimulus which is used to trigger the reaction, it is possible to classify different kind of chemical luminescence: chemiluminescence (CL) and bioluminescence (BL) are referred to the chemical production of light started by mixing the reagents, the latter exploiting enzymes and photoproteins isolated from living organisms [36]; electrogenerated chemiluminescence (ECL) is the luminescence generated by relaxation of exited state molecules produced during an electron-transfer reaction that occurs at the surface of an electrode [37]; thermochemiluminescence (TCL) is the emission of light produced by the thermally-induced decomposition of a molecule.

In order to realize the ideal conditions that allow the production of light through a chemical reaction, it is necessary that you meet the following requirements [38]:

1. The free energy requirements needed to populate the electronically excited state (singlet) via an exergonic process, must meet the following mathematical relationship:

$$-\Delta G \geq \frac{hc}{\lambda_{\text{ex}}} = \frac{28600}{\lambda_{\text{ex}}}$$

Therefore, chemiluminescence reactions producing photons in the visible (400–750 nm) range require around 40–70 kcal mol^{-1}.

2. This electronically excited state has to be accessible on the reaction coordinate.

3. The radiation decay from the excited state to the ground state of the species involved in the reaction has to be a favorable energy release route. This means that either the product of the reaction has to be fluorescent or – if by energy transfer – an excited state can be populated (this energy transfer can occur intra- or intermolecularly).

The chemical luminescence quantum yield is defined as the number of photons emitted per reacting molecule, and depends on the chemical yield of the reaction (Φ_R), the fraction of the product entering the excited state (Φ_{ES}) and the fluorescent quantum yield (Φ_F) as shown in the following relationship:

$$\Phi_{CL} = \Phi_R \, \Phi_{ES} \, \Phi_F$$

One of the most studied systems in chemiluminescence, is the production of photons following the oxidation reaction of luminol in presence of H_2O_2. Luminol can be considered a diprotic acid with pK_A of 6 and 13, respectively. During the CL reaction under basic conditions in presence of H_2O_2, luminol is oxidized to luminol radical anion in its excited state, which releases a photon while decaying to the ground state (Figure 3). The light is emitted at 428 nm (blue light emission) with a relatively low quantum yield of 1% [39]. The reaction can be catalyzed by horseradish peroxidase (HRP) that is commonly used as a label in binding assays thanks to its signal amplification capability [40]
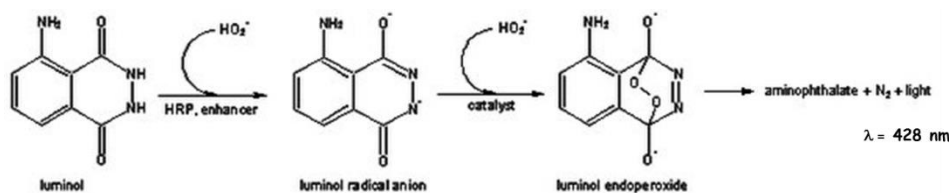
Figure 3: HRP-catalyzed oxidation of luminol.

The possibility to use an enzyme like horseradish peroxidase (HRP) or alkaline phosphatase (AP) as a label allows to amplify the CL signal, since in the presence of an excess of CL substrate many product molecules are generated from one enzyme molecule [41]. Moreover, the achievement of a steady-state of the CL emission allows the standardization of the experimental conditions and quantitation of the labeled probe under investigation, since the steady-state light intensity is directly related to the enzyme activity. To improve the analytical performance of the HRP-catalyzed CL oxidation of luminol, it is possible to add to the CL cocktail some enhancers like p-iodophenol (PIP), 4- (1-imidazolyl)phenol, [42] and other p-phenol derivatives, [43] para-phenylphenol and sodium tetraphenylborate as synergistic enhancer, [44] or $K_3Fe(CN)_6$ as electron mediator [45]. These enhancers allow to amplify and stabilize the CL signal making it easier to measure the analytical signal. The chemiluminescence production of photons with no need for photoexcitation, as it occurs in fluorescence detection, thereby avoiding problems arising from light scattering, background fluorescence or light source instability, makes it a very interesting analytical detection techniques. Therefore, instrumentation for chemical luminescence measurements is in principle very simple, since no excitation source is required. So the integration of this detection technique within portable imaging detection systems such as charge coupled device (CCD) or complementary metal-oxide semiconductor (CMOS) cameras, flexible configurations of the reading

cell (e.g., the spatial distribution of microarray spots on a functionalized surface) makes very simple to realize miniaturized portable lab-on-chip and point of care devices. Finally, chemical luminescence detection showed wide dynamic ranges, thus facilitating analysis of samples with very different analyte concentrations.

1.5 Enzyme in analytical chemistry

As discussed so far, the incorporation of a biological assay into smartphone platforms is a potentially powerful development of new biosensing. In analytical chemistry, a good biosensor is an analytical system that permits a selective and sensitive measurement, but at the same time is easy to handle with low cost. Therefore, in addition to the transducer, which has the task to convert chemical reaction products into processable signals, great importance and attention in the development of a biosensor is dedicated to the biocomponent which is embedded in the device. The biocomponent determines the degree of specificity of the biosensor, as it reacts specifically with an analyte or substrate. Biospecific recognition of the analyte provides the analytical data of interest. And for this reason, the combination of this specificity, with a sensitive transducer, gives to biosensors their unique and unrivalled characteristics for the detection of a variety of analytes in complex matrices. The different components of a biosensor are shown in figure 4.
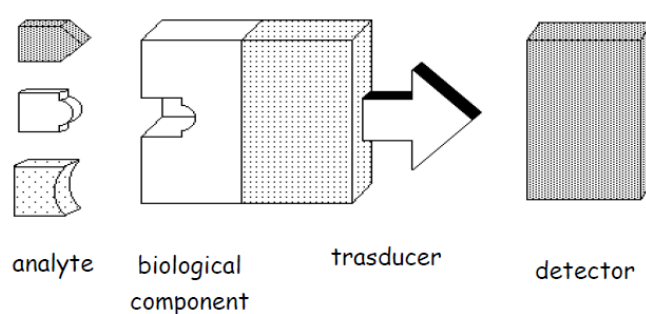
Figure 4. Principle of a biosensor

The principle of operation of a biosensor is very simple: the biological element interacts with the substrate following a specific recognition of the

analyte. A system of transduction converts the biochemical response into an electrical signal. Finally, the signal is processed and amplificated.
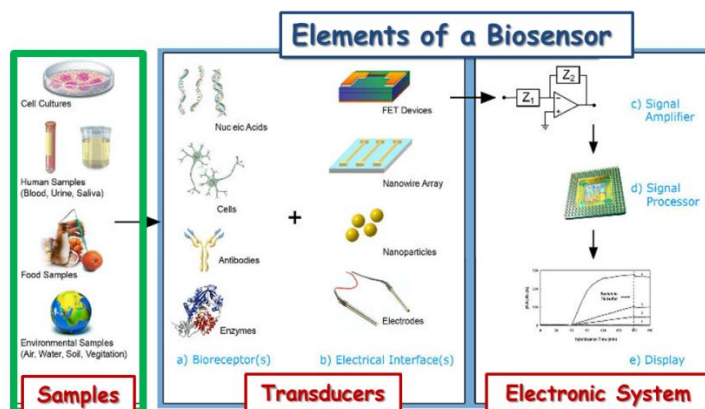
Figure 5. Elements of a biosensor

The recognition component, often called bioreceptor, uses biomolecules from organisms or receptors modeled after biological systems to interact with the analyte of interest. High selectivity for the analyte among a matrix of other chemical or biological components is a key requirement of the bioreceptor. Biosensors can be classified according to common types bioreceptor interactions involving: antibody/antigen, enzymes, nucleic acids/DNA, cellular structures/cells, or biomimetic materials.

The first application of an enzyme in development of a biosensor was carried out by Updike and Hicks [46]. They proposed for the first time in 1967 the term "enzyme electrode" based on entrapped glucose oxidase in a polyacrilamide gel, thus increasing the operation stability of the enzyme and simplifying the sensor preparation. As early as 1970, Clark patented the sequential coupling of two enzymes for the determination of disaccharides [47]. Other biosensors were developed using this type of reaction sequence which was wide spread in metabolism.

1.5.1. Definition of Enzyme

Enzymes are biological catalysts, which increase the rate of biological reactions without themselves being consumed in the reaction. Enzymes are found in all tissues and fluids of the body. Intracellular enzymes catalyze the reactions of metabolic pathways. Enzymes increase reaction rates sometimes by as much as one million fold, but more typically by about one thousand fold. Enzymes increase reaction rates by decreasing the amount of energy required to form a complex of reactants that is competent to produce reaction products. This complex is known as the activated state or transition state complex for the reaction. The free energy required to form an activated complex is much lower in the catalyzed reaction. Enzyme activity is the amount of substrate converted to product per unit time under specific reaction conditions for pH and temperature. Specific activity is defined in terms of enzyme units per mg enzyme protein. Turnover number, related to V_{max}, is defined as the maximum number of moles of substrate that can be converted to product per mole of catalytic site per second. V_{max} is the rate of enzyme activity in saturated concentration of substrate [48].

1.5.2 Michaelis-Menten kinetics

In typical enzyme-catalyzed reactions, reactant and product concentrations are usually hundreds or thousands of times greater than the enzyme concentration. Consequently, each enzyme molecule catalyzes the conversion to product of many reactant molecules. In biochemical reactions, reactants are commonly known as substrates. The catalytic event that converts substrate to product involves the formation of a transition state, and it occurs most easily at a specific binding site on the enzyme. This site, called the catalytic site of the enzyme, has been evolutionarily structured to provide

specific, high-affinity binding of substrate(s) and to provide an environment that favors the catalytic events. The complex that forms, when substrate(s) and enzyme combine, is called the enzyme substrate (ES) complex. Reaction products arise when the ES complex breaks down releasing free enzyme. Between the binding of substrate to enzyme, and the reappearance of free enzyme and product, a series of complex events must take place. An ES complex must be formed; this complex must pass to the transition state (ES*); and the transition state complex must advance to an enzyme product complex (EP). The latter is finally competent to dissociate to product and free enzyme. The series of events can be shown thus:

E + S <---> ES <---> ES* <---> EP <---> E + P

The kinetics of simple reactions like that above were first characterized by biochemists Michaelis and Menten [48]. The Michaelis-Menten equation is a quantitative description of the relationship among the rate of an enzyme-catalyzed reaction [V], the concentration of substrate [S] and two constants, V_{max} and K_M.

$$V = \frac{Vmax\ [S]}{Km+[S]} \qquad \text{(eq 1.1)}$$

Where:

V is the reaction rate

V_{max} is the maximum reaction rate

[S] is the substrate concentration

K_M is the Michaelis-Menten constant

The latter is an algebric statement of the fact that, for enzymes of the Michaelis-Menten type, when the observed reaction rate is half of the maximum possible reaction rate, the substrate concentration is numerically equal to the Michaelis-Menten constant. In this derivation, the units of K_M are those used to specify the concentration of S, usually molarity. A typical Michaelis-Menten plot (graphical analysis of reaction rate (V) versus substrate concentration [S]) is shown in figure 6. The Michaelis-Menten equation is used to demonstrate that at the substrate concentration that produces exactly half of the maximum reaction rate, i.e., $1/2\ V_{max}$, the substrate concentration is numerically equal to K_M.
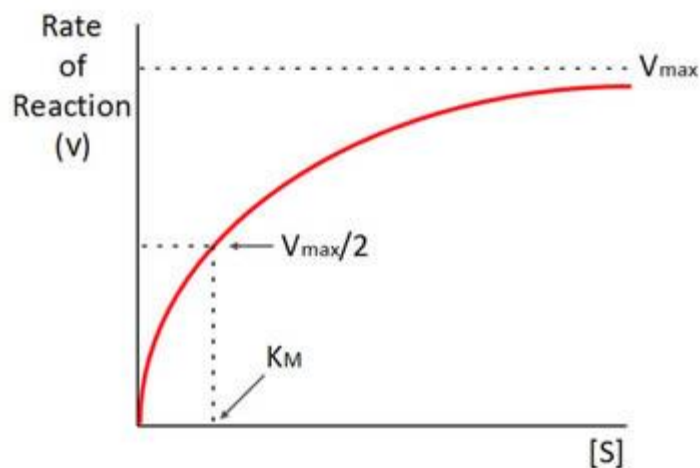
Figure 6. Michaelis-Menten plot

At high substrate concentrations the rate of the reaction is almost equal to V_{max}, and the difference in rate at nearby concentrations of substrate is almost

negligible. If the Michaelis-Menten plot is extrapolated to infinitely high substrate concentrations, the extrapolated rate is equal to V_{max}. When the reaction rate becomes independent of substrate concentration, or nearly so, the rate is said to be zero order. (Note that the reaction is zero order only with respect to this substrate. If the reaction has two substrates, it may or may not be zero order with respect to the second substrate). The very small differences in reaction velocity at substrate concentrations around point C (near V_{max}) reflect the fact that at these concentrations almost all of the enzyme molecules are bound to substrate and the rate is virtually independent of substrate. At lower substrate concentrations, such as at points A and B, the lower reaction velocities indicate that at any moment only a portion of the enzyme molecules are bound to the substrate. In fact, at the substrate concentration denoted by point B, exactly half the enzyme molecules are in an ES complex at any instant and the rate is exactly one half of V_{max}. At substrate concentrations near point A the rate appears to be directly proportional to substrate concentration, and the reaction rate is said to be first order.

To avoid dealing with curvilinear plots of enzyme catalyzed reactions, biochemists Lineweaver and Burk introduced an analysis of enzyme kinetics based on the following rearrangement of the Michaelis-Menten equation [48]:

$$\frac{1}{V} = \frac{Km}{Vmax[S]} + \frac{1}{Vmax} \qquad \text{(eq 1.2)}$$

Plots of 1/V versus 1/[S] yield straight lines having a slope of K_M/V_{max} and an intercept on the ordinate at $1/V_{max}$ (figure 7).
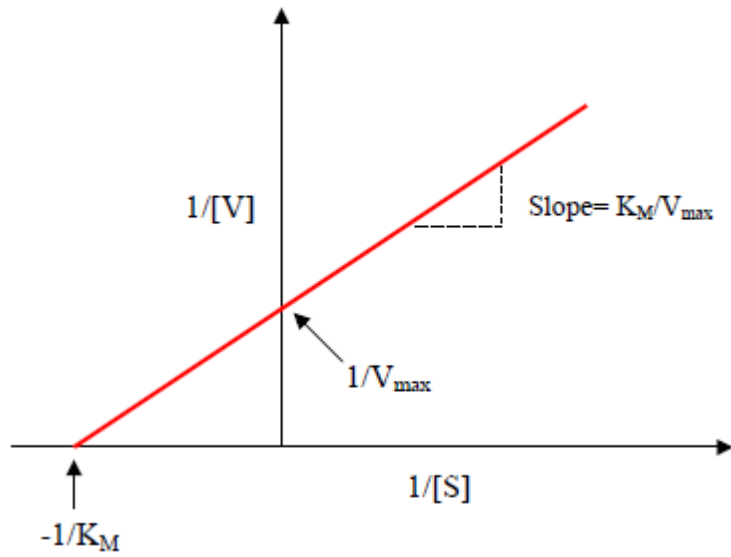
Figure 7. Lineweaver- Burk plot

An alternative linear transformation of the Michaelis-Menten equation is the Eadie-Hofstee transformation:

$$V = Vmax - \frac{KmV}{[S]} \qquad \text{(eq 1.3)}$$

and when V/[S] is plotted on the y-axis versus V on the x-axis, the result is a linear plot with a slope of $-1/K_M$ and the value V_{max}/K_M as the intercept on the y-axis and V_{max} as the intercept on the x-axis. Both the Lineweaver-Burk and Eadie-Hofstee transformation of the Michaelis-Menton equation are useful in the analysis of enzyme inhibition.

1.5.3 Enzyme based biosensors.

The enzyme-based biosensors are widely used, thanks to the wide availability of enzymes that catalyze the reactions of many substrates, to their specificity and catalytic properties. The classes of enzymes, integrated with different transducers to construct biosensors for applications in clinical, veterinary, medical and pharmaceutical areas, food and fermentation processes, environmental monitoring and defense applications [49]. To expand the applications of these biosensors and measuring molecules specific for enzymes that do not belong to the classes mentioned above, it is possible to build a cascade system of coupled enzymes. The primary product of the conversion of the analyte is further converted enzymatically with the formation of measurable secondary product [50][51]. The aim of those who fabricate an enzyme-based biosensor is obtaining a operationally stable biosensor for long term use in monitoring systems, and this characteristic is closely connected to enzyme stability. In order to improve the stability of enzymes, many different techniques have been employed; such as protein engineering [52], the use of enzymes from naturally thermostable microorganisms [53][54], immobilized enzymes [55][56] and by addition of stabilizing agents to the enzymes [57][58].

Table 1. Enzyme based biosensors for various analytes.

Analyte	Enzymes	Transducer
Glucose	GOD	O_2
Sucrose	Invertase, Mutarotase & GOD	O_2 H_2O_2
Amino acids	Amino acid oxidase	O_2
Organophosphorous pesticides	Butyryl cholinesterase	H^+
Morphine	Morphine dehydrogenase	Electron mediator
Urea	Urease	Optical
Metal ions	Urease	Optical

1.5.4 Immobilization of enzymes for stability.

The biological component, usually, fixed closely to the surface of the transducer, influences and shapes the long term stability and reliability of the biosensor. To preserve the biosensor and improve its performance, when you want to use a enzyme-based biosensor, we must pay attention to the conservation and working conditions, in particular, to improve storage stability and operational stability of enzymes, biological component in biosensors. To meet these requirements, it is often necessary to fix the enzyme on a solid support, usually placed near the transducer. The literature is rich of procedures which describe in detail the conditions for immobilizing different biological components to develop a biosensor.

Even if the principles of stabilization of enzymes by means of immobilization for biotechnological applications are well documented [59][60][61], specific practicals and difficult aspects with respect to biosensor applications is insufficient and inadequate. Indeed, some experimental procedures to stabilize and fix a certain enzyme can't be applied to all kind of enzymes belonging to the same classes and depend also by the specific analytical application as well as pH, temperature and environmental conditions. For example, lipase immobilized on ion exchange resins shows better stability in organic solvents [62], but the same is not true in aqueous media which is important for biosensor applications. On the other hand, methods which are widely used for biosensor applications like immobilization by using carbon paste and direct immobilization by activating electrode surface may not be suitable for other biotechnological applications. The development of methods for immobilizing an enzyme without affecting the stability and preserve the catalytic activity, is a critical point in the fabrication of a biosensor and requires a thorough study of the effects related to temperature, pH and denaturants.

1.5.5 Methods of immobilization of enzymes.

Enzyme immobilization methods can be distinguished into two main classes: physical and chemical methods. The main advantage to fix the enzyme to a carrier material or inorganic support, is the improved stability of immobilized enzyme in respect to the enzyme free in solution.
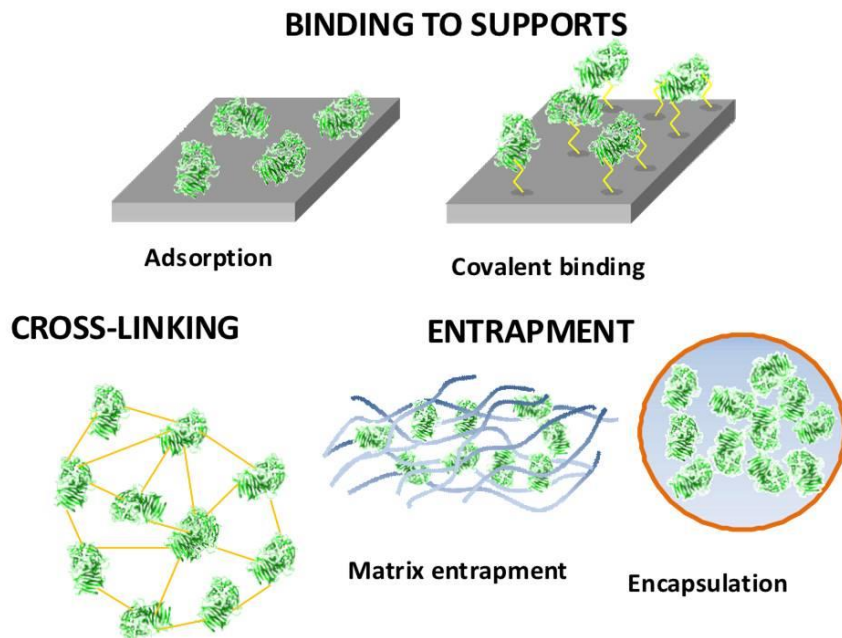
Figure 8. Scheme of enzyme immobilisation methods

Table 2. Common immobilization methods for biosensor construction

Method	Advantages	Disadvantages
Adsorption (physical)	No modification of biocatalyst, matrix can be regenerated, low cost	Binding forces are suceptible to change in pH, temperature and ionic strength, poor stability
Entrapment (physical)	Only physical confinement of the biocatalyst near the transducer	High diffusion barrier, low stability
Covalent bonding (chemical)	Low diffusional resistance, stable under adverse conditions	Harsh treatment by toxic chemicals, matrix not regeneratable
Cross-linking (chemical)	Loss of biocatalyst is minimum, moderate cost, can be prepared in desired shapes	Harsh treatment of biocatalyst by toxic chemicals

1.5.5.1 Physical methods.

Physical methods of immobilization does not require chemical modification of the enzyme, so it is particularly suitable to avoid the risk of inactivating the enzyme. Physical methods of immobilization may be again divided into two classes.

1.5.5.1.1 Adsorption

The adsorption of an enzyme onto a water insoluble material is the simplest method for obtaining enzyme-support conjugates. The solution of bio-molecules is put in contact with the active carrier material for a defined period of time. Thereafter, the molecules that are not adsorbed are removed by washing. . Since the adsorption is regulated by Van der Walls forces, a

change of pH, ionic strength, temperature, etc., may detach the bio-molecules from the carrier.

1.5.5.1.2.Entrapment.

In physical entrapment techniques, enzymes are introduced during the solidification/crosslinking stage of the matrix. Disadvantages of this method are the irregular pore size of the gel, lack of mechanical strength and diffusional limitations encountered by substrate and products. The disadvantages connected to this method are low sensitivity, poor lower detection limit and also poor stability of the biosensor.

1.5.5.2 Chemical Methods.

In these methods of immobilization, enzymes are chemically modified and coupled to carrier with the help of bi- or multifunctional reagents. There are many amino acid side chains that are amenable to chemical modifications of the enzyme. Depending on the nature of chemical modification, chemical methods are divided into two classes: Covalent coupling and Crosslinking.

1.5.5.2.1 Covalent coupling.

In covalent coupling, usually, first the water-insoluble support is activated, to which enzyme is then coupled. The reactive sites on the protein surface can be used for the coupling of the enzyme to the solid support. The surface of the inorganic support must be derivatized before activation. Most used molecules

as bridge between the inorganic and organic interface are: organosilanes like amino propyl triethoxysilane, marcapto propyl trimethoxysilane or glycidoxy propyl trimethoxysilane. Advantages of the use of covalent immobilization of enzymes, are that these immobilized enzyme preparations can be fabricated in sheets, beads, or membranes, which makes this method very useful for industrial and analytical applications. The most significant disadvantage is the relatively low recovery of the enzyme activity. This technique is particularly used to functionalized the electrode surface by a direct immobilization of the enzymes on the electrode. The amount of enzyme loaded on the electrode surface is small and may require a highly sensitive base sensor. These factors limit the application of immobilization by covalent coupling.

1.5.5.2.2 Covalent crosslinking method.

Biopolymers may be intermolecularly cross-linked by bi- or multi-functional reagents. The protein molecules may be cross-linked each other or with another functional protein (for example bovine serum albumine). Glutaraldehyde, bisisocyanate derivates, and bisdiazobenzidine are used as bifunctional reagents. The advantages of cross-linking are the simple procedure and the strong chemical binding of the biomolecules. The main drawback is the possibility of activity losses due to chemical alterations of the catalytically essential sites of protein.

References

[1] W. Hersh, J. A. Jacko, R. Greenes, J. Tan, D. Janies, P. J. Embi, and P. R. O. Payne; (2011) Nature; 470 (7334): 327–329

[2] R. Bercich, J. Bernhard, K. Larson, and J. Lindsey; (2011) IEEE Trans. Biomed. Eng.; 58 (3): 759–762

[3] C. Greenhill; (2012) Nat. Rev. Gastroenterol. Hepatol.; 9 (618)

[4] N. R. Pollock, J. P. Rolland, S. Kumar, P. D. Beattie, S. Jain, F. Noubary, V. L. Wong, R. A. Pohlmann, U. S. Ryan, and G. M. Whitesides; (2012) Sci. Transl. Med., 4 (152)

[5] E. Wang, D. J. Meier, R. M. Sandoval, V. E. Von Hendy-Willson, B. M. Pressler, R. M. Bunch, M. Alloosh, M. S. Sturek, G. J. Schwartz, and B. A. Molitoris; (2012) Kidney Int.; 81 (1): 112–117

[6] F. B. Myers and L. P. Lee; (2008) Lab Chip; 8 (12): 2015–2031

[7] C. H. Ahn, J.-W. Choi, G. Beaucage, J. H. Nevin, J. Lee, A. Puntambekar, and J. Y. Lee; (2004) Proc. IEEE; 92 (1): 154–173

[8] S. C. Kazmierczak; (2011) Clin. Chem.; 57 (9): 1219–1220

[9] S. Wang, F. Xu, and U. Demirci; (2110) Biotechnol. Adv.; 28 (6): 770–781

[10] E. Aguilera-Herrador, M. Cruz-Vera, M. Valcarel; (2010) Analyst; 135: 2220-2232

[11] P. Von Lode; (2005) Clin. Biochem.; 38: 591–606

[12] M. Mirasoli, M. Guardigli, E. Michelini, A. Roda; (2014) J Pharmaceut Biomed; 87: 36-52

[13] D. Lee, W.P. Chou, S.H. Yeh, P.J. Chen, P.H. Chen; (2011) Biosens. Bioelectron. 26: 4349-4354

[14] D. N. Breslauer, R. N. Maamari, N. A. Switz, W. A. Lam, D. A. Fletcher; (2009) PloS ONE, 4: e6320

[15] D. Tseng, O. Mudanyali, C. Oztoprak, S. O. Isikman, I. Sencan, O. Yaglidere, A. Ozcan; (2010)Lab Chip. 10: 1787–1792

[16] O. Mudanyali, S. Dimitrov, U. Sikora, S. Padmanabhan, I. Navruza, A. Ozcan, (2012) Lab Chip. 12: 2678–2686

[17] V. Oncescu, M. Mancuso, D. Erickson; (2014) Lab Chip. 14: 759–763

[18] P. Preechaburana, M. C. Gonzalez, A. Suska, D. Filippini; (2012) Angew. Chem. 124: 11753 –11756

[19] D. Gallegos, K. D. Long, H. Yu, P. P. Clark, Y. Lin, S. George, P. Natha, B. T. ; (2013) Lab Chip. 13: 2124–2132

[20] R. D. Stedtfeld, D. M. Tourlousse, G. Seyrig, T. M. Stedtfeld, M. Kronlein, S. Price, F. Ahmad, E. Gulari, J. M. Tiedje, S. A. Hashsham; (2012) Lab Chip. 12: 1454–1462

[21] https://xone.vodafone.it/product/floome

[22] https://www.breathometer.com

[23] http://www.ihealthlabs.com/glucometer/ihealth-align

[24]http://www.ihealthlabs.com/glucometer/wireless-smart-gluco-monitoring-system

[25] P. B. Lillehoj, M.-C. Huang, N. Truong, C.-M. Ho; (2013) Lab Chip, 13: 2950–2955

[26] L. Shen, J.A. Hagen, I. Papautsky; (2012) Lab Chip. 12: 4240-4243

[27] Q. Wei, R. Nagi, K. Sadeghi, S. Feng, E. Yan, S.J. Ki, R. Caire, D. Tseng, A. Ozcan; (2014) ACS Nano. 8: 1121–1129

[28] S.K. Vashist, E. Marion Schneider, R. Zengerle, F. von Stetten, J.H. Luong; (2015) Biosens. Bioelectron. 66: 169-76

[29] S. Lee, G. Kim, J. Moon; (2013) Sensors. 13: 5109-5116

[30] L.P.V. Cardoso, R.F. Dias, A.A. Freitas, E.M. Hungria, R.M. Oliveira, M. Collovati, S.G Reed, M.S Duthie, M.M.A. Stefani; (2013) BMC Infec. Dis. 13: 497-507

[31] S. Choi, S. Kim, J.S. Yang, J.H. Lee, C. Joo, H.I. Jung; (2014) Sensing and Bio-Sensing Research. 2: 8–11

[32] S. Lee, V. Oncescu, M. Mancuso, S. Mehta, D. Erickson; (2014) Lab Chip. 14: 1437–1442

[33] V.K. Rayendran, P. Bakthavathsalam, B.M.J. Ali; (2014) Microchim. Acta. 181: 1815-1821

[34] A.F. Coskun, R. Nagi, K. Sadeghi, S. Phillips, A. Ozcan; (2013); Lab Chip. 13: 4231-4238

[35] A.I. Barbosa, P. Gehlot, K. Sidapra, A.D. Edwards, N.M. Reis; (2015) Biosens. Bioelectron. 70: 5–14

[36] A. Roda A., M. Guardigli; (2012) Anal Bioanal Chem 402: 69–76

[37] L. Hu, G. Xu; (2010) Chem Soc Rev; 39: 3275–3304

[38] Chemiluminescence and Bioluminescence: Past, Present and Future, Edited by Aldo Roda, Royal Society of Chemistry 2011, Published by the Royal Society of Chemistry

[39] R. Creton, L. F. Jaffe; (2001) BioTechniques; 31: 1098-1105

[40] Roda A., Pasini P., Guardigli M., Baraldini M., Musiani M., Mirasoli M., Fresenius J., (2000) Anal Chem; 366, 752-759

[41] Dotsikas Y., Loukas Y. L.; (2004) Anal Chim Acta; 509: 103-109

[42] Dotsikas Y., Loukas Y. L.; (2007) Talanta; 71: 906-910

[43] Luo J. X., Yang X. C.; (2003) Anal Chim Acta; 485, 57-62

[44] Chouhan R. S., Babu K. V., Kumar M. A., Neeta N. S., Thakur M. S., Rani B. E. A., Pasha A., Karanth N. G. K., Karanth N. G.; (2006) Biosen Bioelectron; 21: 1264-1271

[45] Marzocchi E., Grilli S., Della Ciana L., Prodi L., Mirasoli M., Roda A.; (2008)Anal Biochem; 377: 189–194

[46] Updike S.j., Hicks G.P. Nature 214 (1967) 986.

[47] Clark L.C. (1965) US Patent 4040 908.

[48]Matthews C.K., Van Holde K.E., Ahern K.G. (2004) 3rd edition Ambrosiana, Milan.

[49] Guilbault, G.G. (1984) Analytical uses of immobilized enzymes, Marcel Dekker Inc. New York USA, pp 160.

[50] Xu, Y., Guilbault, G.G. and Shia, S.K. (1989) Anal. Chem., 61, 782.

[51] Scheller, F. and Renneberg, R. (1983) Anal. Chim.Acta. 152, 265.

[52] Nosoh, Y., Sekiguchi, T. (1993) Thermostability of enzymes (Ed. Gupta, M.N.) Springer, Berline. pp 182.

[53] McNail, C.J., Spoors, J.A., Cocco, D., Cooper, J.M. and Bannister, J. V. (1989) Assay.Anal. Chem.61, 25.

[54]Rain, C.A., Aurin, S.D., Guagliardi, A., Bartolucci, S., DeRosa, M. and Ross, M. (1995)Biosensor. Bioelectron. 10, 135.

[55] Scouten, W.H., Luong, J.H.T. and Broun, S. (1995) TIBTECH. 13, 178.

[56] Kullary, K.M.R., Lee, W.E. and Thompson, M. (1992) Anal. Chem. 64,1063.

[57] Gibson, T.D., Higgins, I.J. Woodward, J.R. (1992) Analyst. 117, 1293.

[58] Gibson, T.D., Hulbert, J.N., Woodward, J.R. (1993) Anal. Chim. Acta. 279, 185. [59] Farahdiba, J., Husain, S. and Saleemuddin, M. (1993) Biotechnol. Appl. Biochem. 18, 401

[60] Gupta, M.N. (1991) Biotechnol. Appl. Biochem. 14,1.

[61] Klibanov, A.M. (1979) Anal. Biochem. 93, 1

[62] Turner, N.A., Duchateau, D.B. and Vulfson, E.N. (1995) Biotech. Lett. 17, 371

CHAPTER 2

SMARTPHONE EMBEDDED ENZYMATIC CHEMILUMINESCENCE-BASED BIOSENSOR FOR POINT-OF-NEED APPLICATION: SMARTCHOL

2.1 Introduction

Today, smartphones are not just phones, but are real miniaturized portable computers. They have several functions through which it is possible to meet users' needs and are finding wide use not only in recreational activities, but also in health and medicine. Thanks to the development of new apps and adding accessories, smartphones built-in functions and capabilities can be further extended. The extensive distribution of smartphones and tablets, together with cloud services ensuring pervasive connectivity, creates an incredible market, largely untapped, especially in the field of healthcare self-management.[1] The integration of smartphone camera as detector into point-of-care (POC) analytical devices allow to realize a new evolution POC devices to perform tests outside clinical laboratories, even in low resource settings for critical and emergency medicine. Exploiting the multiple smartphone capabilities, it is possible to have an "all-in-one device". Unlike existing biosensor technologies smartphone-based biosensor eliminate the need for separate devices and, after running the analytical test, processed data could be stored, or sent by E-mail to a physician to properly manage the diagnosis and follow-up, thus facilitating the new approach of "personalized medicine".[2]

In literature a lot of examples have been recently reported showing the use of smartphone-based platforms to detect biomarkers and analytes of clinical interest in bodily fluids including sweat, blood, and saliva.[3,4] The smartphone camera has been previously used exploiting detection principles such as colorimetric measurements,[5–7] fluorescence,[8] and label-free formats.[9] To the best of our knowledge, chemiluminescence (CL) has not yet been implemented as detection principle for smartphone-based biosensing.

In this work, for the first time, chemiluminescence (CL) is implemented as detection principle for smartphone-based biosensing. The main advantage of CL is the high sensitivity of technique that allows to improve the analytical performance of bioassays and measure down to 10^{-15}–10^{-18} moles of the target analyte in a small volume or spot.[10] Cooled charge-coupled device (CCD) is a suitable portable and compact device for the detection of proteins down to attomole levels and nucleic acids at femtomole levels.[11] Although their sensitivity is still lower than cooled CCDs,[12] back-illuminated complementary metal-oxide semiconductors (BI-CMOS) integrated into smartphones could be suitable for the measurement of analytes present at medium-abundant concentrations (e.g., at micromolar levels) using CL detection. Coupled CL enzymatic reactions have been previously used to increase the sensitivity in comparison to conventional colorimetric substrates. Analytical assay based on CL coupled enzymatic reaction involves the use of oxidase enzymes such as glucose oxidase, cholesterol oxidase, urate oxidase that produce hydrogen peroxide, which, in turn, can be detected by the CL reaction with luminol and enhancers, catalyzed by horseradish peroxidase (HRP).[13] The aim of this work is, for the first time, the use of smartphone camera as detector to image and quantify chemiluminescence coupled biospecific enzymatic reactions to measure analytes in blood. Using low-cost 3D printing technology[17] we fabricated a smartphone accessory and a minicartridge for hosting biospecific reactions. As a proof-of-principle we develop a smartphone-based assay to quantify serum total cholesterol using cholesterol esterase/cholesterol oxidase in which the produced H_2O_2 is detected using the CL of the luminol– H_2O_2–HRP system.

2.2 Materials and Chemicals.

Peroxidase type VI-A from horseradish 1080 units/mg, 3α-HSD, recombinant cholesterol oxidase from Brevibacterium sp. 50 units/mg protein, cholesterol esterase from Pseudomonas fluorescens ($\sim$20% protein), hydrogen peroxide. Super Signal West Dura Extended Duration substrate was obtained from Thermo Scientific (Waltham, MA, USA). Blood membranes LF1 and Whatman No.1 filter paper were purchased from Whatman International, Ltd. (Maidstone, England).

2.3 Smartphone Camera Characterization.

The smartphone used as CL detector has been an Iphone 5S (Apple, Cupertino, CA, USA) with a BI-CMOS sensor and 8-megapixel (8MP) camera. To evaluate the detection capabilities and sensitivity of smartphone camera, a comparative study has been performed by analyzing standard solutions of H_2O_2 by CL reaction with the smartphone camera and a thermoelectrically cooled MZ-2PRO CCD camera (MagZero, Pordenone, Italy) equipped with a Sony ICX285 image sensor (1360 × 1024 pixels, pixel size = 6.45 μm × 6.45 μm) that has been previously reported by us.[11] Briefly, a series of standard solutions of the system H_2O_2/luminol/enhancer/HRP with a concentration of hydrogen peroxide ranging from 0.01 μM to 10 mM where the reagents are adsorbed on a disk 4 mm in diameter were analyzed and the images collected with the two instrumentations (Figure 1). The images have been processed with ImageJ software to measure the signal over the sample spot area and expressed as relative light units (RLUs).

Figure 1. (a) Thermoelectrically cooled MZ-2PRO CCD camera (MagZero) equipped with a Sony ICX285 image sensor (1360 x 1024 pixels, pixel size 6.45 x 6.45 µm^2) (b) Iphone 5s with BI-CMOS sensor and 8MP camera.

2.4 3D-Printed Smartphone Accessory Device Fabrication.

The assay minicartridge and the mini darkbox smartphone accessory were fabricated using the low cost 3D-printing technology. In particular have been used a dual-extrusion 3D printer Replicator 2X (Makerbot, Boston, MA, USA), and a thermoplastic black acrylonitrile butadiene styrene polymer as fabrication material. To create three-dimensional (3D) models have been used the open-source Tinkercad browser-based 3D design platform (Autodesk, Inc.). MakerWare v.2.4 software, which uses an algorithm that slices digital files (exported as .stl files) into thin layers for 3D printing, was used to define printing options and settings.

Figure 2. (a) Picture of the accessory, (b) picture of the minicartridge, and (c) picture of the accessory snapped into the smartphone. (d) Schematic cutaway drawings of the minicartridge showing the integration of the various components. The transparent ABS optical window (200 μm) of 4 mm diameter allows imaging of biochemiluminescent reaction. (e) Introduction of the minicartridge into the accessory and (f) picture of a representative CL acquisition with the smartphone.

The device accessory is composed of of two main parts: a phone adapter comprising the darkbox and lens holder and a cartridge for the bioassays (Figure 2). The depicted accessory, complementary as external housing accessory for the Iphone 5S, holds a plano-convex lens 6 mm in diameter (Edmund Optics, York, U.K.) in contact with the phone objective and a mini-cartridge (3.5 cm length, 1.2 cm width, and 5 mm thickness) with an optical window of 4 mm diameter, made by a thin layer (200 μm) of transparent acrylnitrile butadiene styrene (ABS, from Amazon.co.uk) deposited exploiting the dual-extrusion printing option. The disposable mini-cartridge contains a blood separator pad holder, with a LF1 glass fiber filter, connected to a reaction chamber where a 4 mm nitrocellulose disk supporting the specific enzymes is placed. A separate 15 μL reservoir for CL reagents is connected via microfluidics to the reaction chamber at 200 μm height in order to prevent premature mixing. The minicartridge consists of two separate pieces, which are then glued together, in order to insert the specific supports and solutions.

2.5 Sample Collection.

Microsafe collection and dispensing tubes (with preset volume of 15 μL) were used for fingerprick sampling and dispensing of whole blood into the minicartridge.

2.6 Total Cholesterol Smartphone-Based Assay (SmartChol).

The assay principle consists in coupling three enzymatic reactions: (1)

esterified cholesterol hydrolysis by cholesterol esterase, (2) cholesterol oxidation by cholesterol oxidase, and (3) CL detection of the produced hydrogen peroxide using Super Signal West Dura Luminol/ Enhancer solution in the presence of HRP as a catalyst.

The optimized assay conditions are the followings: the enzymes (1U cholesterol oxidase, 0.5U cholesterol esterase, and 0.05U HRP) have been co-absorbed on the nitrocellulose disk (4 mm diameter), while a reagents' reservoir contains the CL reagent (15 μL). A volume of 15 μL of blood is inserted into the minicartridge from the back inlet by touching the exposed pad. Within 2 min, the serum is directed toward the reaction chamber, where enzymatic reactions take place. CL reaction is triggered 3 min after sample injection with a simple flick in order to drive the CL reagent from the reservoir to the reaction chamber. The minicartridge is then inserted into the smartphone mini darkbox accessory and the light signal measured by the smartphone camera for 30 s using LongExpo app (Eyetap Soft LLC). To process the CL images and obtained quantitative results has been used ImageJ software v.1.46 (National Institutes of Health, Bethesda, MD). Regions of interest (ROIs) corresponding to the detection chamber and back-ground were selected and light emissions quantified as raw integrated densities. GraphPad Prism (GraphPad Software, Inc., La Jolla, CA) was used to plot CL signal as a function of total serum cholesterol concentration. Cholesterol Trinder assay (FAR Diagnostics, Verona, Italy) was used to evaluate accuracy of SmartChol. The standard solution of 200 mg/dL cholesterol contained in the kit was concentrated via rotary evaporation to obtain cholesterol solutions in the range of 140–386 mg/dL that were added to charcoal-stripped serum.

2.7 Results and Discussion

The simple accessory developed in this work was designed with the aim of using the smartphone camera as a luminometer, to measure the light produced by CL systems coupled with analyte specific enzymatic reactions.

2.7.1 Smartphone Camera Analytical Performance.

New generation smartphones use BI-CMOS photodiodes as light sensors to increase light collection with reduced size. Compared to the conventional front-illuminated light sensors, this architecture allows one to reduce the pixel pitch and increase the optical efficiency,[12] making mobile devices suitable to detect very weak light signals, such as those produced by CL reactions, with reasonable exposure time (e.g., few seconds, minutes).

A comparative study using a lensless cooled CCD camera, previously reported by us,[11] and an iPhone 5S, showed that the BI-CMOS is less sensitive but still adequate to measure the photons produced by CL reactions and to detect analytes present at concentrations from the micromolar level to the millimolar level, with the advantage of being integrated in a smartphone . For this purpose, a series of standards solutions of the system H_2O_2/luminol/enhancer/HRP with a concentration of hydrogen peroxide ranging from 0.01 µM to 10 mM were analyzed and the images collected with the two instrumentations (Figure 1). In terms of resolution, the images obtained with the smartphone camera show better performance thanks to the inclusion of a plano-convex lens to focus the image. In this configuration, two spots of 4 mm diameter at a distance of 1 mm can be simultaneously imaged without cross-talk, fitting the smartphone display size.
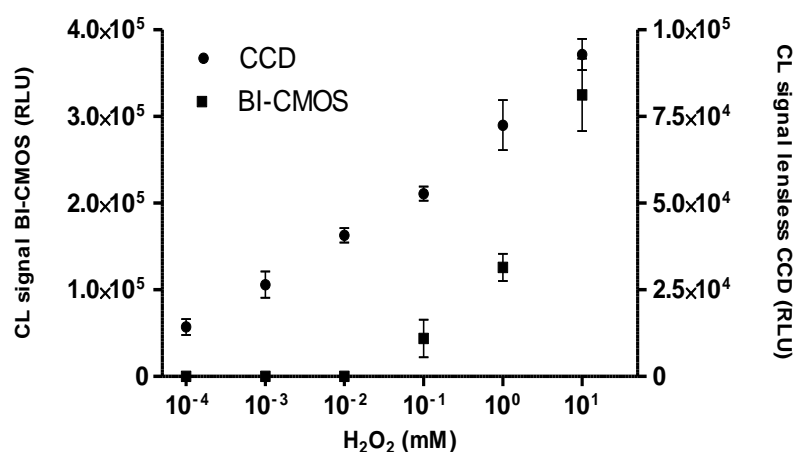
Figure 3. Chemiluminescence calibration curves for a series of standards solutions of the system H_2O_2/luminol/enhancer/HRP.

Concerning detectability, even if the cooled CCD is able to image and quantify a concentration of H_2O_2 three decades lower, the BI-CMOS detector is suitable for detecting analytes present in biological fluids at micromolar levels, as the majority of common biomarkers of clinical interest.

2.7.2 3D-Printed Accessory Device.

We fabricated a compact smartphone accessory and a minicartridge for specific enzymatic reactions using a desktop 3D printer obtaining rapidly several prototypes, avoiding to realize for each one a master, such as with polydimethylsiloxane (PDMS) protocols. In addition, physical 3D models were quickly generated with a printing time of ~10 min for the minicartridge and 30 min for the accessory. 3D models were easily designed using computer-aided design (CAD) programs, converted to Stereo Lithography (.stl) file format and elaborated with a slicer software that allows the 3D object to be printed as subsequent layers of thermoplastic material at a defined horizontal resolution. ABS, which becomes moldable at 220–230 °C, was used as printing material. We chose to use an affordable yet versatile 3D printer that

allows one to print objects with two different colors or materials in order to develop more-sophisticated devices with less printing steps. This feature was exploited to create a 200-μm thin transparent ABS-based window over the minicartridge reaction chamber allowing the acquisition of CL signals while preventing any leakage. The constructed smartphone accessory device can be easily snapped to the smartphone, providing a minidarkbox for the minicartridge.

2.7.3 Total Cholesterol Quantification by Smartphone-Based Assay (SmartChol).

The smartphone-based assay (SmartChol) quantifies the total cholesterol in 15 μL of whole blood by exploiting cholesterol esterase and cholesterol oxidase that produces cholest-4-en-3-one and H_2O_2. The hydrogen peroxide is then measured reacting with luminol, enhancers, and HRP as a catalyst, producing light emission of CL reaction. In the minicartridge there are: a pad for one-step serum separation from whole blood, a nitrocellulose disk in which the enzymes, i.e., cholesterol esterase, cholesterol oxidase, and HRP, are co-adsorbed and a reservoir containing Super Signal West Dura for CL reaction. The ABS hydrophobicity and channel width avoid that no accidental release of the reagents occurs. In order to achieve the highest CL signal with a reasonably stable kinetics, different conditions were optimized including pH and concentrations of enzymes and reagents. Under the optimized conditions, the CL signal is proportional to the cholesterol concentration in the sample with a linear range from 20 mg/dL to 386 mg/dL and a limit of detection (LOD) of 20 mg/dL.
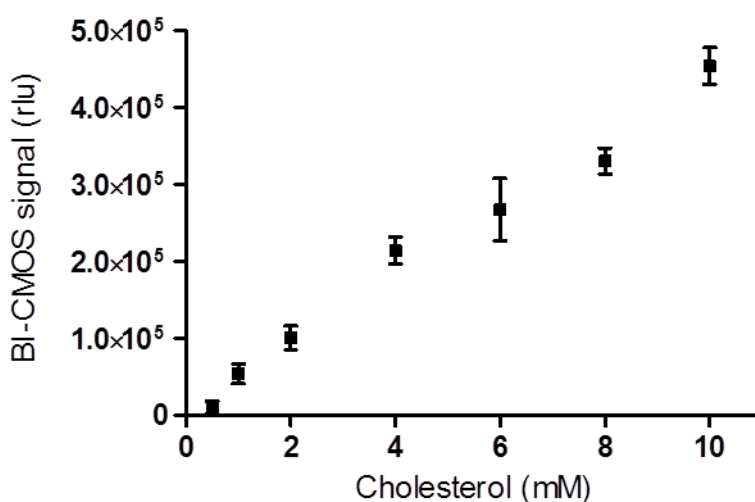

Figure 4. Chemiluminescence calibration curve for cholesterol obtained with standard cholesterol

solutions in phosphate buffer 0.1M, pH 7.0. Data represent the mean value ± SD of three measurements.

Figure 5 shows CL images acquired with the smartphone and quantitative analysis of physiologically relevant cholesterol concentration range (>240 mg/ dL).
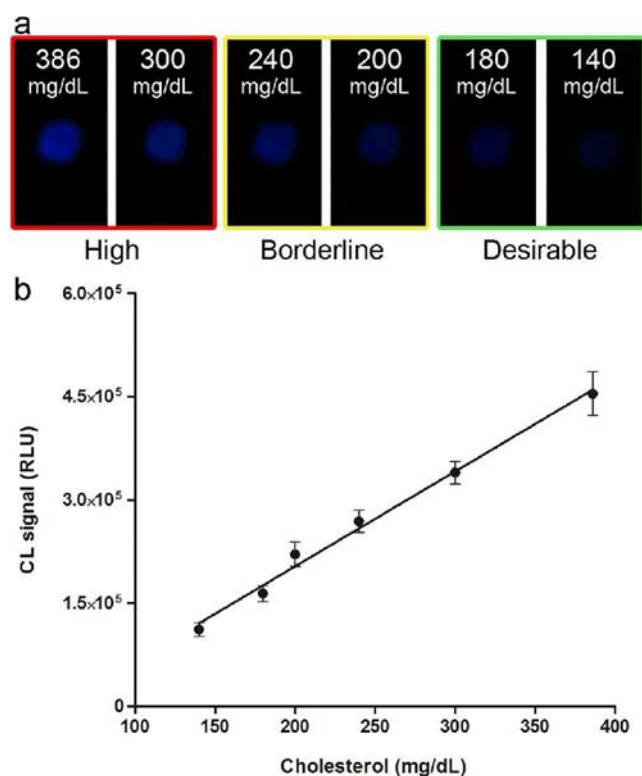
Figure5. (a) Raw BL images of six charcoal-stripped human serum samples spiked with cholesterol measured by the smartphone camera, using the LongExpo app (30 s) showing low, medium, and high cholesterol concentrations. (b) Quantitative analysis of the same samples measured with SmartChol. Data represent the mean values ± the standard deviation (SD) obtained using three different minicartridges.

The accuracy of the smartphone total cholesterol assay was determined by quantifying cholesterol levels in serum samples in the range of 140–386 mg/dL and comparing them to results obtained using a commercial kit. At each concentration, six minicartridges were used and the within-run coefficient of variation was 5% for the sample containing 240 mg/dL

cholesterol. Figure 6 shows the correlation between SmartChol and Trinder method obtained analyzing 10 serum samples of unknown cholesterol concentration (r^2 = 0.996, p < 0.0001). The smartphone-based CL test is able to discriminate and quantify the total cholesterol over the entire range of physiological values. Physiological desirable serum cholesterol levels (<200 mg/dL) are reliably discriminated from border-line-high (200–240 mg/dL) and high risk values.
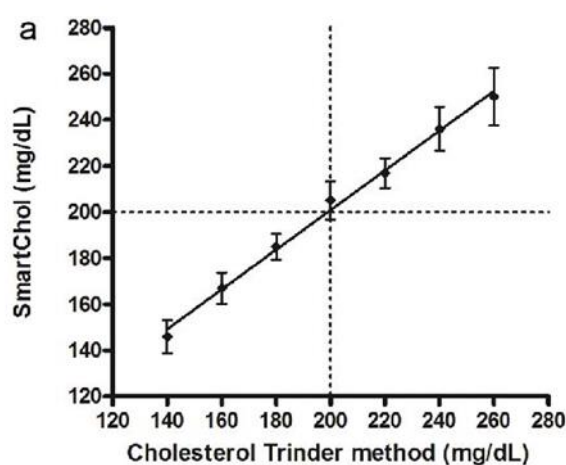

Figure 6. (a) Correlation between SmartChol and Trinder method obtained analyzing 10 serum samples of unknown cholesterol concentration (r^2 = 0.996, p < 0.0001).

As shown by results, SmartChol assay has similar analytical performance when compared to electrochemiluminescence-based cholesterol biosensor (linear range from 0.83 mM to 2.62 mM, detection limit = 0.28 µM).[19] Even if the reported assay having a higher LOD than other amperometric biosensors,[20,21] it has the non-negligible advantage of requiring only a smartphone, thus eliminating the need to have additional detectors or devices for the test with a cost of ~3–5 euros per assay including manufacturing and reagents. The availability of this simple and minimally invasive tool to measure blood cholesterol could be of clinical utility for several diagnostic needs such as the monitoring of subjects with ischemic stroke high risk, post-menopausal women, diabetic children, and, more

generally, to monitor a patient's metabolic status.

2.8 Conclusion

The aim of this work has been to demonstrate, for the first time, that the smartphone camera can be used to image and quantify the light produced by chemiluminescence reactions used to amplify analyte-specific enzymatic reactions. A simple and compact smartphone accessory has been prototyped and fabricated using facile and cost-effective three-dimensional (3D) printing. This accessory has the dual role of acting as a darkbox for shedding from ambient light and hosting the minicartridge, used to perform analytical assay.

The suitability of this accessory was demonstrated with SmartChol for measuring cholesterol in serum. This assay can be performed within 3 min in a very straightforward manner with just few easy actions: snap the accessory onto the smartphone, add sample (e.g., 15 μL of blood) to analyte-specific minicartridge, introduce the minicartridge in the accessory and flick it, wait 3 min, and get results. The SmartChol could find relevant applications in the monitoring of cholesterol levels in children at risk with the possibility to perform the assay in pediatric outpatient clinic, helping the management of childhood obesity.[24] Therefore, potential future applications span from monitoring of pregnancy with cholestasis, to infants with cholestatic jaundice, patients with duodenum gastric reflux, to pharmacological therapy monitoring. The extreme simplicity of the device widens it applicability and makes it suitable for the detection of many analytes of clinical interest, for instance any H_2O_2 producing oxidases such as those specific for glucose, lactate, and ethanol. Therefore, SmartChol could be considered as the forerunners of the integration.

References

(1)   Vashist, S. K.; Mudanyali, O.; Schneider, E. M.; Zengerle, R.; Ozcan, A. Anal. Bioanal. Chem. 2014, 406, 3263–3277.

(2)   Boulos, M. N.; Wheeler, S.; Tavares, C.; Jones, R. Biomed. Eng. Online 2011, 10, 24.

(3)   Lee, S.; Oncescu, V.; Mancuso, M.; Mehta, S.; Erickson, D. Lab Chip 2014, 14, 1437–1442.

(4)   Oncescu, V.; O'Dell, D.; Erickson, D. Lab Chip 2013, 13, 3232– 3338.

(5)   Shen, L.; Hagen, J. A.; Papautsky, I. Lab Chip 2012, 12, 4240– 4243.

(6)   Oncescu, V.; Mancuso, M.; Erickson, D. Lab Chip 2014, 14, 759–763.

(7)   Byoung-Yong, C. Bull. Korean Chem. Soc. 2012, 33 (2), 549.

(8)   Petryayeva, E.; Algar, W. R. Anal. Chem. 2014, 86, 3195–3202.

(9)   Gallegos, D.; Long, K. D.; Yu, H.; Clark, P. P.; Lin, Y.; George, S.; Nath, P.; Cunningham, B. T. Lab Chip 2013, 13, 2124–2132.

(10) Roda, A.; Pasini, P.; Mirasoli, M.; Michelini, E.; Guardigli, M. Trends Biotechnol. 2004, 22, 295–303.

(11)   Roda, A.; Mirasoli, M.; Dolci, L. S.; Buragina, A.; Bonvicini, F.; Simoni, P.; Guardigli, M. Anal. Chem. 2011, 83, 3178–3185.

(12)   Watanabe, N.; Tsunoda, I.; Takao, T.; Tanaka , K.; Asano, T. Jpn. J. Appl. Phys. 2010, 49, 04DB01. DOI: 10.1143/JJAP.49.04DB01.

(13)   Ryan, O.; Smyth, M. R.; Fagáin′, C. O. Essays Biochem. 1994, 28, 129–146.

(14)   Roda, A.; Kricka, L. J.; DeLuca, M.; Hofmann, A.F. J. Lipid Res. 1982, 23, 1354–1361.

(15)   Blum, L. J.; Gautier, S. M.; Coulet, P. R. J. Biotechnol. 1993, 31, 357–368.

(16)   Roda, A.; Girotti, S.; Ghini, S.; Grigolo, B.; Carrea, G.; Bovara, R. Clin. Chem. 1984, 30, 206–210.

(17)   Gross, B. C.; Erkal, J. L.; Lockwood, S. Y.; Chen, C.; Spence, D. Anal. Chem. 2014, 86, 3240–3253.

(18)   Ford, J.; De Luca, M. Anal. Biochem. 1981, 110, 43–48.

(19)   Zhang, J.; Chen, S.; Tan, X.; Zhong, X.; Yuan, D.; Cheng, Y. Biotechnol. Lett. 2014, in press (DOI: 10.1007/s10529-014-1547-9).

(20)   Soylemez, S.; Kanik, F. E.; Ileri, M.; Hacioglu, S. O.; Toppare, L. Talanta 2014, 118, 84–89.

(21) Ruecha, N.; Rangkupan, R.; Rodthongkum, N.; Chailapakul, O. Biosens. Bioelectron. 2014, 52, 13–19.

(22) Jablonski, E.; DeLuca, M. Proc. Natl. Acad. Sci. U. S. A. 1976, 73, 3848–51.

(23) Festi, D.; Morselli, A. M.; Roda, A.; Bazzoli, F.; Frabboni, R.; Rucci, P.; Tavoni, F.; Aldini, R.; Roda, E.; Barbara, L. Hepatology 1983, 5, 707–713.

(24) Vinci, S. R.; Rifas-Shiman, S. L.; Cheng, J. K.; Mannix, R. C.; Gillman, M. W.; de Ferranti, S. D. JAMA 2014, 311, 1804–1807.

CHAPTER 3

A 3D-PRINTED DEVICE FOR A SMARTPHONE-BASED CHEMILUMINESCENCE BIOSENSOR FOR LACTATE IN ORAL FLUID AND SWEAT (SMARTLAC)

3.1 Introduction

Today, smartphones are becoming increasingly popular and are revolutionizing our lifestyles. Their use is no longer limited only to a private and recreational scope. It is used as a means of communication but, thanks to their various functionalities, it is integrated into the way we work. In fact there are many apps that allow us to exchange data and documents at various levels, through mails, bluetooth, internet, social networks. The computing power of smartphones, also allows you to write, edit and process documents and files in all areas. Particular interest is growing towards the development of apps for healthcare delivery, providing medical and diagnostic tools to reserved respond to need of end-users. In September 2013, the Food and Drug Administration (FDA) recommended that apps providing medical and scientific information can be distinguished from those with diagnostic potential.[1] This distinction allows healthcare professionals and policy-makers to identify those apps which fall under the remit of the FDA. In contrast to conventional point-of-care (POC) devices, smartphone-based diagnostics eliminate the need for dedicated equipment. The smartphone itself can act as a transducer or detector and perform data analysis. Smartphones offer photography (still and video), location and other sensors (global positioning system [GPS], accelerometers, etc.), the long-distance transfer of information (data and images) via text messaging (Short Message Service – SMS), built-in apps (e-mail, calendar, document readers, etc.), the possibility of developing or installing new apps, and wireless data service.

It is possible to download or buy a lot of apps specific for health self-management, limited to medication reminders, post-intervention questionnaires, therapy adjustments, and supportive messages for patients

with chronic diseases like diabetes and asthma.[2,3] Exploiting smartphone technology, it is much more challenging to use smartphones as instruments for point-of-need analysis, e.g. immuno- or enzyme-based tests. In literature, there are several examples which demonstrate the feasibility of this approach for monitoring biomarkers in biological fluids such as blood, saliva, and sweat using enzymatic reactions, paper-based immunoassays, and lateral ow immunoassays (LFIAs).[4–6] Mobile phone embedded cameras have already been used for fluorescence or colorimetric detection to measure analytes and detect infectious pathogens in environmental and clinical samples.[7–9] In a recent paper, Oncescu et al. have developed a smartphone accessory and a so ware app for measuring cholesterol levels in blood, based on the colorimetric changes induced by enzymatic reactions on a dry reagent paper strip.[10] Polymerase chain reaction (PCR) has also been integrated into a smartphone-assisted device by combining solar heating with microfluidics.[11] In contrast to fluorescence detection, CL produces photons as a byproduct of a chemical reaction, with no need for a light source. This bypasses problems connected with background fluorescence and light scattering.[12] The main difficulty to be considered for the development of CL smartphone-embedded devices is that, despite the possibility of achieving low detection limits, CL is characterized by very low light emission intensities, especially when compared to fluorescence.[13,14] Therefore, CL detection requires highly sensitive detectors and must be performed in a darkbox to avoid interference from ambient light. The latter inconvenience can be easily solved by adopting a light-proof minicase.

The monitoring of lactate levels is relevant for diabetes control, sport medicine, and for critical-care patients at the risk of heart attack. There is a close relationship between lactate accumulation and muscle fatigue. Reaching

of anabolic threshold can be easily assessed by lactate monitoring. Lactate can be quantified in different biological fluids, including blood, saliva, and sweat.[17] Several lactate biosensors based on different detection principles (chemiluminescence and amperometric detection) have already been realized to evaluate the endurance performance of athletes via lactate monitoring in sweat and blood.

The aim of this work is the development of a smartphone-based device for non-invasive and easy monitoring of the endurance performance of athletes via lactate detection. This biosensor relies on CL detection and exploits the lactate oxidase (LOx) catalyzed reaction coupled with the enhanced luminol/H_2O_2/ horseradish peroxidase (HRP) CL system. The device was fabricated with low-cost 3D printing technology and is composed of a disposable analytical minicartridge, a mini dark box to avoid interference from ambient light during measurement, and a holder to connect the dark box to a smartphone. We have shown that the device could be used for the reliable real-time measurement of lactate levels in oral fluid and sweat samples. In principle, this biosensor could also find applications in detecting other analytes of clinical interest in oral fluid and sweat.

3.2 Materials and methods

3.2.1 Chemicals

Peroxidase (type VI-A from horseradish, 1080 U mg^{-1} protein), L-lactate oxidase (from Pediococcus sp., 50 U mg^{-1} protein), L-lactate sodium salt, L-histidine monohydrochloride mono-hydrate, mucin (type II from porcine stomach) and urea were supplied from Sigma Aldrich (St. Louis, MO). Sodium chloride, disodium hydrogen orthophosphate anhydrous, sodium dihydrogen orthophosphate monohydrate were supplied from Carlo Erba Reagents S.r.l. (Milano, Italy). The luminol-based HRP substrate Super Signal® West Dura was from Thermo Scienti c (Waltham, MA). Artificial sweat was prepared according to the International Standard Organization (ISO105-E04-2008E) and the British Standard (BS EN1811-1999) with a pH 5.5 [0.05% (w/v) L-histidine monohydrochloride monohydrate, 0.50% (w/v) NaCl, and 0.22% (w/v) $NaH_2PO_4 \cdot 2H_2O$].[22] Artificial saliva at pH 7.2 was prepared by dissolving 0.6 mg mL^{-1} Na_2HPO_4, 0.6 mg mL^{-1} anhydrous $CaCl_2$, 0.4 mg mL^{-1} KCl, 0.4 mg mL^{-1} NaCl, 4.0 mg mL^{-1} mucin and 4.0 mg mL^{-1} urea in deionised water according to Tlili et al.[23] The fluorometric lactate enzymatic assay in the standard 96-well microtiter plate format (EnzyFluo™ L-Lactate Assay Kit) was bought from BioAssay Systems, Hayward, CA and used according to the manufacturer's instructions.

3.2.2 Smartphone camera performance comparison

The performance of the smartphone (Samsung Galaxy SII Plus, Samsung Group, Seoul, South Korea) embedded camera was compared with that of a benchtop low-light luminograph equipped with a thermoelectrically cooled CCD camera (LB 981 Night Owl, Berthold Technologies GmbH & Co. KG, Bad Wild-bad, Germany). A battery-powered blue LED (λ_{max} = 466 nm) was used as a model source. To evaluate the response of the cameras to different light intensities, the emission of the LED was attenuated using Kodak Wratten 2 neutral density (ND) filters of known optical density (Edmund Optics, Barrington, NJ). The image exposure time was set to 30 s for both cameras. For evaluation of the signal-to-noise (S/N) ratios of the images, signals (S) were calculated by averaging the pixel intensity over the LED image area, while noise (N) was taken as the standard deviation of the mean pixel intensity in a dark image area.

## 3.2.3 3D printed analytical device fabrication
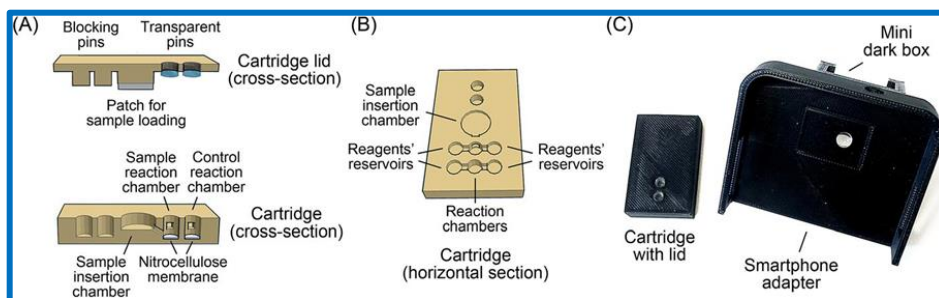
Fig. 1 The 3D printed analytical device made of black and transparent ABS polymers consisting of three separate components: a disposable analytical cartridge (42 mm _ 28 mm) with two reaction chambers, two reagents' reservoirs and a sample chamber, a mini dark box, and a smartphone adapter. (A) Cross-sections of the analytical cartridge and the cartridge lid and (B) the horizontal section of the analytical cartridge showing the internal chambers and fluidic connections. (C) Photo of the cartridge-lid assembly and of the mini dark box and smartphone adapter.

The analytical device (Fig. 1) has been fabricated using as materials the black and transparent acrylonitrile-butadiene-styrene (ABS) polymers and has been printed using a low-cost commercial 3D printer (Replicator 2X Desktop 3D Printer, MakerBot Industries, New York, NY). The device was designed using the open-source Tinkercad browser-based 3D design platform (Autodesk, Inc.). Files were exported as .stl les and MakerWare v.2.4 so ware, an algorithm that slices digital into thin layers for 3D printing, was used to define printing options and settings. The device is composed of three separate components: (a) a disposable analytical cartridge, (b) a mini dark box, and (c) a smartphone adapter. The analytical cartridge (42 mm × 28 mm) contains two reaction chambers (sample and control reaction chamber) (diameter 4 mm, depth 5 mm) with small 4 mm-diameter disks of the nitrocellulose membrane, onto which LOx and HRP are co-absorbed. The enzyme amounts immobilized on the disks were as follows: LOx 1.0 U (for sweat analysis) or 0.02 U (for saliva analysis), horseradish peroxidase 0.1 U. Two reagents' reservoirs adjacent to each reaction chamber (diameter 4 mm, depth 3 mm)

contain the luminol/enhancer solution of the Super Signal® West Dura HRP CL reagent (10 μL) and a 0.1 M, pH 7.0 buffer phosphate solution (10 μL). The buffer reservoir adjacent to the control reaction chamber also contains L-lactate in artificial saliva or sweat matrices (the same volume of the sample analyzed: 15 μL) to provide an adequate control (2.0 mmol L^{-1} and 4.0 mmol L^{-1} lactate for saliva and sweat, respectively). The sample reaction chamber is connected to a sample insertion well (diameter 9 mm, depth 4 mm), by which the biological fluid to be analyzed can be added. The cartridge is covered by a cartridge lid that avoids fluid leakage during storage and use of the cartridge. The lid can be fitted on the cartridge in two different orientations. When the cartridge is not in use, two lid pins are inserted in the reaction chambers, blocking the channels connecting the reaction chambers to the reagents' reservoirs and avoiding premature mixing of the reagents. During the analysis, the lid is fitted onto the cartridge in the opposite orientation: the reagents can freely flow from the reservoirs to the reaction chambers and two transparent ABS pins are inserted in the reaction chambers, allowing measurement of the CL emission. The lid holds a further pin with a patch (9 mm diameter, 2 mm thickness) right by the sample insertion well, which allows a fixed volume of sample to be transferred to the sample reaction chamber. The mini dark box contains the analytical cartridge during the measurement, ensuring its correct positioning and avoiding interference from ambient light. The smartphone adapter holds the mini dark box and can be snapped onto the smartphone to correctly position the dark box in relation to the smartphone embedded camera. The adapter includes a plano-convex plastic lens (diameter 6 mm, focus 12 mm), which focuses the image of the reaction chambers of the cartridge onto the smartphone camera.

3.2.4 Assay procedure

Oral fluid and sweat are collected by unsnapping the lid from the cartridge and applying the patch on the lid to the skin of the forearm or forehead or to the tongue, respectively. The lid is then inserted into the cartridge in the measurement orientation by applying a slight pressure. This closes the cartridge and drives a fixed volume of sample (15 μL) into the reaction chamber. The CL enzymatic reaction is then triggered a after sample injection with two simple flicks, which drive the buffer phosphate solution (and the L-lactate standard for the control) and the CL reagent from the reservoirs to the reaction chambers. The cartridge is then inserted into the mini dark box camera, which is already snapped to the smartphone. The light signal is measured by using the smartphone camera. Suitable smartphone photography apps are used to control the exposure time (which must be long enough to achieve the required detectability) and for image handling. For android-based smartphones, we used the Camera FV-5 (Android) Lite app to perform long (60 s) image acquisitions. Quantitative analysis of the CL images was performed using the open source so ware ImageJ v.1.46 (National Institutes of Health, Bethesda, MD). Regions of interest (ROIs) corresponding to the sample and control detection chambers, as well as a ROI of the same dimension in a dark area of each image for subtraction of the background signal, were selected. Light emissions of CL reaction were quantified as raw integrated densities. GraphPad Prism v. 5.04 (GraphPad So ware, Inc., La Jolla, CA) was used to plot the CL signal as a function of lactate concentration and for least-squares fitting of calibration curves.

3.3 Results and discussion

The aim of this work was to develop a portable lactate CL biosensor to measure L-lactate levels in oral fluid and sweat, based on the coupling of the enzymatic oxidation of lactate catalyzed by L-lactate oxidase with the luminol/H_2O_2/HRP CL system. We realized a simple device using disposable analytical cartridges to detect the light photons produced by the enzyme reaction using a smartphone embedded camera. This device exploits the backside-illumination complementary metal-oxide semiconductor (BI-CMOS) sensors integrated into modern smartphones. These offer improved low-light performance in comparison with conventional front-illuminated CMOS sensors. The device also takes advantage of low-cost 3D printing technologies, which allowed the rapid prototyping and production of device components.

3.3.1 Smartphone camera performance

Chemiluminescent reactions produce weak light emissions. An estimation of the light detectability required to satisfy the analytical requirement of the device can be done as follows. According to the L-lactate content of oral fluid with a physio-logical range of 0.1–2.5 mmol L^{-1} and sweat with values that vary up to 25 mmol L^{-1} according to an individual's metabolism and physical performance,[24–26] we need a minimum L-lactate detectability of the order of 0.1 mmol L^{-1}. At this concentration level, a 15 mL sample of biological fluid contains as low as 1 nmole of L-lactate, which will be converted by L-lactate oxidase to the same amount of hydrogen peroxide. Assuming a quantum efficiency of the luminol/H_2O_2/HRP CL system of the order of 0.01, the HRP-catalyzed reaction of the hydrogen peroxide with luminol will produce about

10^{13} photons, which should be imaged and detected by using the smartphone embedded camera. By taking into account the system optics and geometry, it could be estimated that the light collection efficiency of the device (the fraction of the photons emitted by the sample that effectively reach the CMOS sensor) should be of the order of 5%. Finally, by considering that the image of a reaction chamber of the cartridge covers an area of about 2.8×10^5 image pixels, we concluded that the minimum light detect-ability required is around 10^3 photons per image pixel. We preliminarily compared the performance of the smartphone embedded camera to that of a low-light luminograph equipped with a thermoelectrically cooled CCD camera using a model LED light source. Both systems showed a good correlation between measured signals and light intensities. However, for any given intensity of the model light source, the S/N ratios of the luminograph images were about three orders of magnitude higher than those of the images acquired with the smartphone embedded camera (data not shown). Since the S/N ratio determines light detectability, it could be concluded that the minimum light intensity detectable with the smartphone embedded camera is about three orders of magnitude higher than that of the low-light luminograph. The lower light detect-ability of the smartphone embedded camera could be ascribed to several factors, such as the smaller pixels (1.4×1.4 mm^2 vs. 9×9 mm^2) and the absence of a sensor cooling system, which resulted in a higher thermal noise. Nevertheless, the sensitivity of the smartphone camera is still adequate for the quantitative measurement of analytes through enzyme-catalyzed CL reactions, at least for species present at relatively high concentrations, providing a careful optimization of the analytical system.

3.3.2 Analytical device design

The analytical device obtained by low-cost 3D printing technology[27] is designed to be snapped onto a Samsung Galaxy SII smartphone, allowing a simple one-step analytical procedure after introducing a sample into the cartridge. The 3D printing technology allows rapid prototyping of the analytical device (particularly the adapters, which are designed to t a specific smartphone model according to its size and the camera position). In principle, the system could also be adapted to tablets. Due to their larger screens, tablets may be preferable to smartphones for applications requiring image visualization (e.g. cell imaging or lateral ow immunochromatographic analyses). The analytical cartridge is the critical component. It allows a simple one-step analytical procedure in which a defined amount of sample is introduced into the cartridge and mixed with the enzymes and other reactants. Since enzyme reactions (thus CL emission intensities) are affected by temperature and other environmental variables, the cartridge includes a suitable control to improve assay accuracy and reproducibility.

To fulfill these requirements, all the reagents required for the analysis are already contained in the analytical cartridge, either in the reagents' reservoirs or, in the case of the enzymes LOx and HRP, immobilized in the dry state on a nitrocellulose membrane. The analytical cartridge contains two separate reaction chambers (each of them connected to its own reagents' reservoirs), in which the sample and a lactate control are analyzed in parallel. For quantitative analysis, the CL signal of the sample is normalized to that of the control (2.0 mmol L^{-1} or 4.0 mmol L^{-1} lactate for oral fluid or sweat, respectively). In addition, the control sample is prepared in artificial oral fluid or artificial sweat to take into account the effect of the sample matrix on the

intensity of the CL signal. The whole analytical procedure is simply controlled by acting on the cartridge lid. Removal of the lid allows the reagents to ow from the reservoirs to the reaction chambers. The lid is also used for collecting and transferring oral fluid or sweat samples: upon collection of the sample in the lid patch, inserting the lid into the cartridge drives a fixed volume of sample (15 μL) into the sample reaction chamber. Afterwards, shaking the cartridge transfers the reagents into the reaction chambers and initiates the enzyme reactions leading to light emission.

3.3.3 Assay optimization.

Due to the relatively low sensitivity of the embedded smart-phone cameras, experimental conditions (enzymes concentrations, pH, sample volumes, etc.) were optimized to provide a strong CL signal and a relatively fast emission kinetics.

3.3.4 Enzyme immobilization.

The enzymes required for the assay enzymes were co-absorbed on small nitrocellulose membrane disks (diameter 4 mm) placed in the reaction chambers of the analytical cartridge. Nitrocellulose membranes are commonly used for protein absorption because of their high binding capacity and low background staining, and because physical immobilization of enzymes on membranes is easy and does not affect enzyme activity as much

as covalent bonding or cross-linking methods. The enzyme amounts were optimized to obtain intense CL signals and fast reaction kinetics (rapid conversion of lactate into pyruvate and H_2O_2 followed by the HRP-catalyzed oxidation of luminol by H_2O_2) even in the presence of large amounts of lactate. Because of the higher lactate concentrations in sweat, different optimal amounts of LOx were individuated for the two matrices: cartridges for sweat analysis were loaded with a larger amount of LOx (1.0 U) than those for analysis of oral fluid (0.02 U). But both cartridges contained the same amount of HRP (0.1 U).

3.3.5 Emission kinetics.

 To achieve a low detection limit, it was necessary to collect a large fraction of the light emitted by the CL enzyme reaction. In addition to optimizing the geometry of the device, a suitable integration time was selected for acquiring the CL signal from the cartridge. The analysis of the kinetic pro les of the CL emission in the presence of different amounts of lactate showed the light emission kinetics emission slightly depended on the concentration of lactate. The maximum emission intensities were obtained at times varying from 15 s (for the lowest lactate concentrations) to 30 s (for the highest ones) upon introduction of the sample and triggering of the enzymatic reactions (Fig. 2). According to the kinetics of the reaction, an integration time of 60 s upon insertion of the cartridge into the device was chosen to collect at least 90% of the overall light emission independently from the lactate concentration of the sample.
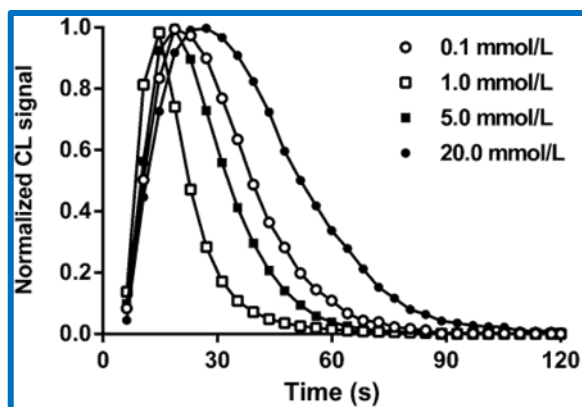
Fig. 2 Chemiluminescence kinetic profiles obtained for the analysis of artificial sweat samples containing different lactate concentrations in the range 0.1–20 mmol L^{-1}. Kinetics measurements were performed by imaging the analytical cartridge using an electron multiplying charge coupled device (EM-CCD) camera (ImagEM-X2, Hamamatsu, Japan)

3.3.6 Matrix effect.

To perform a reliable measurement of lactate in real samples, the possible interference of oral fluid and sweat matrices on the CL signal was evaluated. To study the matrix effect, we compared the CL emissions obtained for samples with low (1 mmol L^{-1}) and high (8 mmol L^{-1}) lactate levels prepared in artificial oral fluid (or sweat) and in phosphate buffer. The sample matrices caused a significant decrease of the intensity of the CL signal (about 60–70% and 40% for oral fluid and sweat, respectively). A similar reduction of the CL signal was also observed by analyzing real samples prepared by spiking oral fluid and sweat samples with negligible (less than 0.1 mmol L^{-1}) lactate concentrations with known amounts of lactate. To take into account the matrix effect, the calibration curves used for the quantitative analysis of lactate, as well as the control samples in the cartridges, were obtained using lactate solutions prepared in artificial oral fluid and sweat. This allowed a reliable evaluation of lactate concentrations in real samples as reported below.

3.3.7 Analytical performance
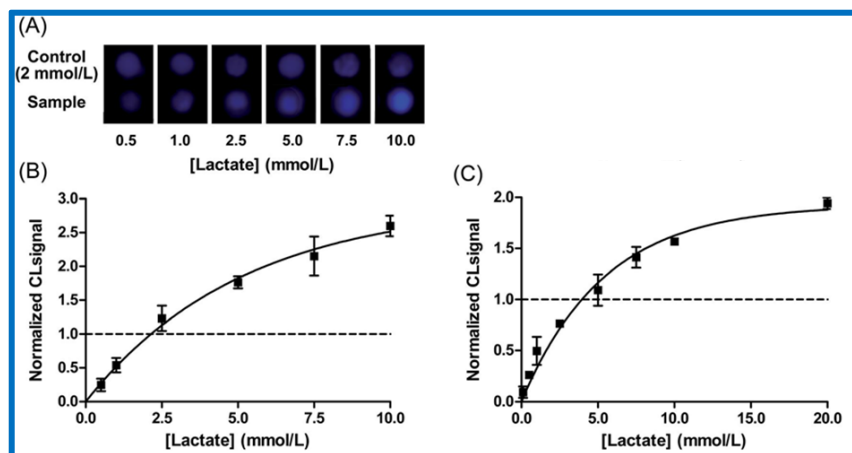
Fig. 3 (A) Images obtained by analyzing lactate standard solutions in artificial oral fluid and calibration curves obtained in (B) oral fluid and(C) sweat. Chemiluminescence signals were normalized to the CL signals obtained for the control samples (2.0 and 4.0 mmol L^{-1} for oral fluid and sweat, respectively) of the same cartridge. The least-square fitting of the experimental data according to the empirical equation $y = a(1 - e^{-bx})$ is also shown ($R^2 = 0.98-0.99$). Data points represent the mean ± SD of three replicates.

Fig. 3B and 3C show the calibration curves obtained by analyzing standard lactate solutions prepared in artificial oral fluid and sweat following the optimized analytical procedure described above. Each measure was performed in a separate cartridge and the CL signal obtained for the sample was normalized to the value recorded for the control (2.0 and 4.0 mmol L^{-1} for oral fluid and sweat, respectively) in the same cartridge. Signal normalization is expected to increase assay reproducibility by reducing the effect of environmental variables (e.g. temperature) and other factors on the intensity of the CL signal. The CL signal showed a nonlinear dependence on the lactate concentration. To perform quantitative analysis, calibration curves were obtained by fitting the experimental data with the empirical equation $y = a(1 - e^{-bx})$, where y and x represent the CL signal and the lactate concentration, respectively. According to the calibration curves, limits of detection (LOD) of 0.5 mmol L^{-1} (corresponding to 4.5 mg dL^{-1}) and 0.1 mmol

L^{-1} (corresponding to 0.9 mg dL^{-1}) of lactate were obtained in oral fluid and sweat, respectively. In addition, the smartphone-based lactate biosensor allowed measurement of lactate in oral fluid and sweat along the entire range of physiological values.

3.3.8 Assay validation

To validate the assay, oral fluid and sweat samples were analyzed in parallel with the smartphone-based lactate biosensor and with a commercial L-lactate enzymatic assay based on the lactate dehydrogenase-catalyzed oxidation of lactate, in which the formed NADH reduces a probe into a highly fluorescent product. Fluorescence detection allowed us to achieve a LOD (1 mmol L^{-1}) lower than that of colorimetric lactate enzymatic assays. Samples could thus be analyzed upon dilution to avoid any matrix effect. Fig. 4 compares the concentrations measured in oral fluid and sweat samples, which indicated a good correlation between the effective concentration of lactate in the samples and the results obtained with the smartphone-based lactate biosensor.
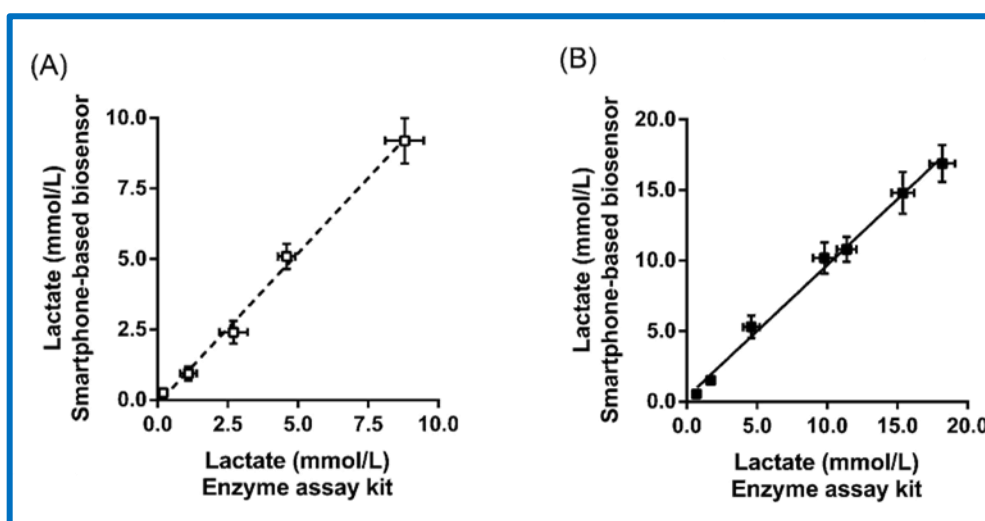

Fig. 4 Comparison of the lactate concentrations measured in (A) oral fluid and (B) sweat samples using the smartphone-based lactate biosensor and a fluorometric L-lactate enzymatic assay kit performed in the standard 96-well microtiter plate format (EnzyFluo™ L-Lactate Assay Kit). Each data represents the mean ± SD of three replicates.

3.3.9 Application

Lactate levels increase during intense physical exercise, thus they are an indicator of performance development in training regimes, especially endurance sports. To demonstrate the applicability of the smartphone-based biosensor for monitoring lactate levels during physical exercise, we measured the lactate in sweat during the running track performed by a volunteer. Fig. 5 shows the sweat lactate pro le measured in the volunteer and obtained by collecting and immediately analyzing sweat sampled at regular intervals (10 minutes). The data clearly showed the increase in lactate concentration during the exercise activity, demonstrating the possibility of real-time monitoring of lactate levels.
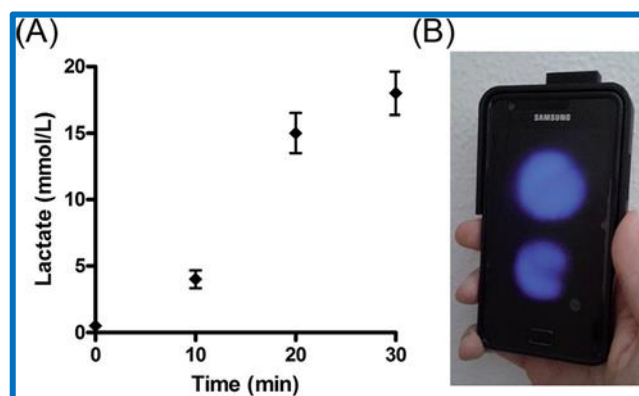

Fig. 5 (A) Lactate concentrations in sweat measured in real-time during the exercise activity performed by a volunteer (each data represent the mean _ SD of three replicates). Sweat samples, collected by unsnapping the lid from the cartridge and applying the patch on the lid to the skin of the forearm or forehead, were taken at 10 min intervals and immediately analyzed. (B) Picture of a representative CL acquisition with the smartphone.

Measurement of lactate in sweat or oral fluid also allowed assessment of the athlete's anaerobic threshold, i.e. the exercise level above which pyruvate production due to anaerobic metabolism is faster than pyruvate consumption due to aerobic metabolism. Above this threshold, accumulation of unused

pyruvate and its conversion into lactate causes acidosis, reducing exercise endurance. Instead of performing a lactate quantitative analysis to assess the reaching of the anaerobic threshold, the CL signal obtained for the sample could simply be compared to that of the internal control, providing that the lactate concentration in the control corresponded to the anaerobic threshold level in sweat or oral fluid. As an example of this approach, Fig. 6 shows the results obtained using cartridges containing a 4.0 mmol L^{-1} lactate control sample for the analysis of sweat samples with lactate concentrations of about 2.0 and 8.0 mmol L^{-1}, respectively. In accordance with the calibration curves, the CL signal intensities were not linearly proportional to the analyte concentration. But sweat samples with lactate concentrations below and above the control sample could easily be discriminated. This approach could therefore allow a simple assessment of the reaching of the anaerobic threshold by an athlete as a result of continual exercise at high intensity. However, the lactate level corresponding to the anaerobic threshold may present a significant inter individual variation, which will also depend on the fitness of the subject. This approach may therefore require the development of a series of cartridges, in which control samples cover a range of lactate concentrations.
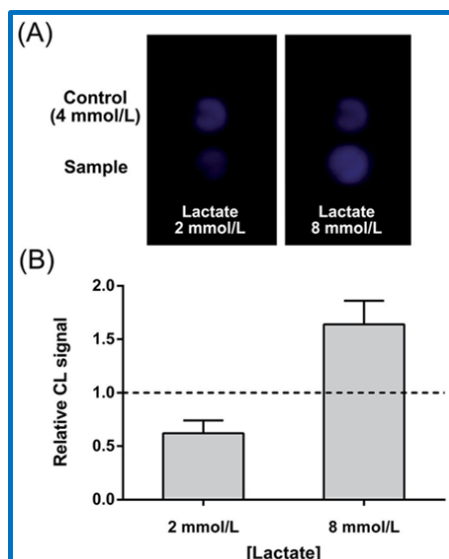
Fig. 6 (A) CL images of cartridges with a 4.0 mmol L^{-1} lactate control obtained for the analysis of sweat samples with lactate concentrations of 2.0 and 8.0 mmol L^{-1}. Sweat samples were assayed in the lower reaction chamber, while control samples were analyzed in the upper one. (B) Relative CL signals of the sweat samples (normalized to the CL signal of the control, mean ± SD of three replicates)

3.3.10 Conclusions

We have demonstrated the possibility to integrate chemiluminescence detection principle smartphone's camera detector and 3D printing technology to realize a sort of new revolutionary and very simple "portable mini-laboratory". The most important element of this mini-lab is a disposable plastic cartridge for enzymatic assays and a smartphone accessory that can be easily tailored to different smartphones and tablets. As proof-of-concept, we developed an assay to monitor lactate levels in sweat and oral fluid. This device shows adequate analytical performance, offering a cost-effective alternative for non-invasive lactate measurement to monitor the intensity and the maximum duration of athletes' performance during physical exercise.

The device could also be adapted to a variety of other assays that require simplicity, low-cost, portability, and flexibility. The data reported in this work clearly demonstrate that using chemiluminescence-based analytical assay and a smartphone camera as a luminometer is an ideal strategy for developing simple, sensitive, and portable analytical devices. In addition, ad hoc applications can easily be implemented to process the image and elaborate the test results, providing the end user with a simple readout (e.g. analyte concentration in comparison with physiological ranges or a sort of "traffic light"). This smart test could activate a green light when the analyte is within physio-logical values (personalized to the individual according to results stored in the memory), amber light when concentrations are reaching the threshold, and red light (or a voice alert warning) for higher values. Moreover, the device could be used to monitor lactic acidosis to prevent heart attacks in critical-care patients.

References

1 Food and Drug Administration, Mobile medical applications: guidance for industry and Food and Drug Administration staff, http://www.fda.gov/downloads/ MedicalDevices/./UCM263366.pdf.

2 T. de Jongh, I. Gurol-Urganci, V. Vodopivec-Jamsek, J. Car and R. Atun, Cochrane Database Syst. Rev., 2012, 12, CD007459.

3 S. Silow-Carroll and B. Smith, Issue Brief. (Commonw Fund.), 2013, 30, 1–10.

4 L. Sangdae, K. Giyoung and M. Jihea, Sensors, 2013, 13, 5109– 5116.

5 V. Oncescu, M. Mancuso and D. Erickson, Lab Chip, 2014, 14, 759–763.

6 D. Erickson, D. O'Dell, L. Jiang, V. Oncescu, A. Gumus, S. Lee, M. Mancuso and S. Mehta, Lab Chip, 2014, 14, 3159–3164.

7 G. H. Chen, W. Y. Chen, Y. C. Yen, C. W. Wang, H. T. Chang and C. F. Chen, Anal. Chem., 2014, 86, 6843–6849.

8 E. Petryayeva and W. R. Algar, Anal. Chem., 2014, 86, 3195– 3202.

9 C. Stemple, S. V. Angus, T. S. Park and J. Y. Yoon, J. Lab. Autom., 2014, 19, 35–41.

10 V. Oncescu, D. O'Dell and D. Erickson, Lab Chip, 2013, 13, 3232–3238.

11 L. Jiang, M. Mancuso, Z. Lu, G. Akar, E. Cesarman and D. Erickson, Sci. Rep., 2014, 20, 4137–4141.

12 A. Roda, M. Guardigli, E. Michelini and M. Mirasoli, Anal. Bioanal. Chem., 2009, 393, 109–123.

13 C. A. Marquette, B. P. Corgier and L. J. Blum, Bioanalysis, 2012, 4, 927–936.

14 S. Pennathur and D. K. Fygenson, Lab Chip, 2008, 8, 649–652.

15 A. Roda, L. Cevenini, S. Borg, E. Michelini, M. M. Calabretta and D. Schuler,¨ Lab Chip, 2013, 13, 4881–4889.

16 A. Roda, E. Michelini, L. Cevenini, D. Calabria, M. M. Calabretta and P. Simoni, Anal. Chem., 2014, 86, 7299–7304.

17 G. G. Guilbault, G. Palleschi and G. Lubrano, Biosens. Bioelectron., 1995, 10, 379–392.

18 P. J. Lamas-Ardisana, O. A. Loaiza, L. Anorga, E. Jubete, M. Borghei, V. Ruiz, E. Ochoteco, G. Cabanero and H. J. Grande, Biosens. Bioelectron., 2014, 56, 345–351.

19 H. Nakamura, Y. Murakami, K. Yokoyama, E. Tamiya, I. Karube, M. Suda and S. Uchiyama, Anal. Chem., 2001, 73, 373–378.

20 A. Hemmi, K. Yagiuda, N. Funazaki, S. Ito, Y. Asano, T. Imato, K. Hayashi and I. Karube, Anal. Chim. Acta, 1995, 316, 323–327.

21 M. M. Rahman, M. J. Shiddiky, M. A. Rahman and Y. B. Shim, Anal. Biochem., 2009, 384, 159–165.

22 K. Kornphimol, S. Sujittra, B. Kanittha, K. Wiyong and M. Rawiwan, Part. Fibre Toxicol., 2010, 7, 1–9.

23 C. Tlili, L. N. Cella, V. N. Myung, V. Shetty and Mulchandani, Analyst, 2010, 135, 2637–2642.

24 N. W. Tietz, Clinical Guide to Laboratory Tests, W.B. Saunders Company, Philadelphia, PA, 3rd edn, 1995.

25 J. M. Green, R. C. Pritchett, T. R. Crews, J. R. McLester Jr and D. C. Tucker,

Eur. J. Appl. Physiol., 2004, 91, 1–6.

26 W. Jia, A. J. Bandodkar, G. Vald´es-Ram´ırez, J. R. Windmiller, Z. Yang, J. Ram´ırez, G. Chan and J. Wang, Anal. Chem., 2013, 85, 6553–6560.

27 B. C. Gross, J. L. Erkal, S. Y. Lockwood, C. Chen and D. M. Spence, Anal. Chem., 2014, 86, 3240–3253.

CHAPTER 4

COLOR-BASED SMARTPHONE APPLICATIONS

4.1 Color Theory

For physics, color is a set of values, it is a graph that represents the amount of energy reflected from a surface at wavelength varying. But the human eye is not able to enter so much information for each individual color. The eye makes a summary measure of the components around the blue, green and red, according to the sensitivity curves of the cones of the retina (Figure1).
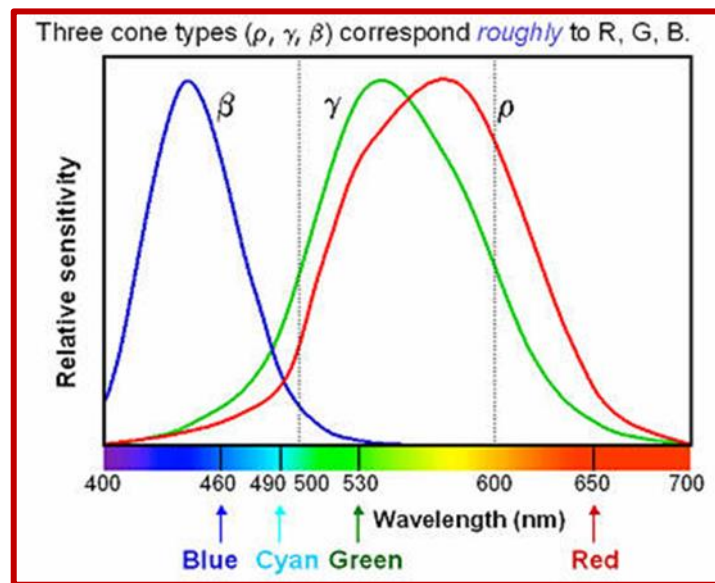

Figure 1. Human spectral sensitivity to color

The color is an elaboration of the brain human. The measurement of color can not only be based on the comparison performed from the eye of an average observer between the color assumed by the surface under consideration, when it is illuminated with a white light source standards, and the color assumed by a perfectly white surface(ie, with a coefficient of reflectance ideally equal to 100% at any wavelength) illuminated, in turn, by three lights with the basic colors (Figure 2): red, green, blue intensity values of a surface of interest, can be quantified in comparison with those of a reference surface. Indeed, according to the theory of the tristimulus, any color can be reproduced exactly by a suitable mixture of the three basic colors (Figure 3).
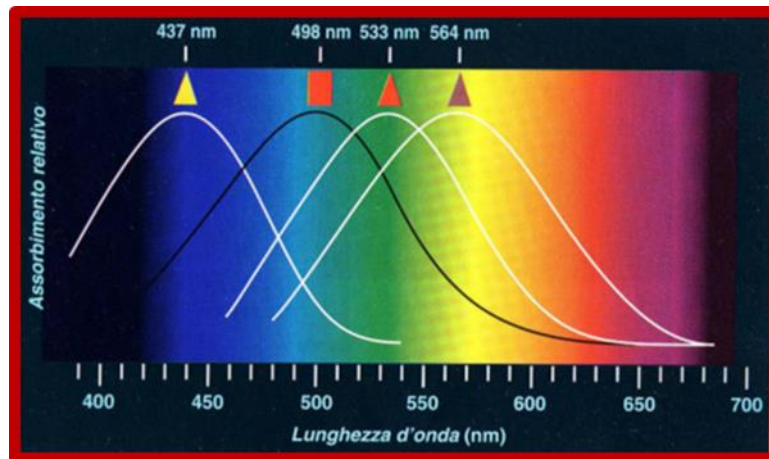
Figure 2. Curves of relative sensitivity (in white) of the three types of cones in the human eye in blue and red with green maximum values of wavelength indicated. The black curve indicates the relative sensitivity of the other kind of receptors: rods of eyes. The sensitivity threshold of the rods is much smaller than that of the cones. This explains because the human eye perception of vision is very low in presence of dimmed lighting conditions.

The wavelengths of the three fundamental colors correspond to the values of maximum sensitivity of the eye in the red, in green and in the blue for the three types of specific receptors of each color exist in the retina (cones). The color that each of us perceives is produced by the intensity of nerve impulses, separately transmitted to the brain by the three types of cones.

In general, the sum of different colors produces an additive color and the phenomenon is called additive synthesis. Exists also subtractive synthesis that, instead, consists in subtracting colors corresponding to certain wavelengths from the spectrum of white. This is achieved by using partially opaque or, equivalently, partially transparent materials, such as colored glass, with which are produced the optical filters. So crossing some filters, it is possible to obtain other colors. For example, the yellow filter suppresses the blue. The filter that suppresses the green, is magenta (or purple), and the filter that suppresses red appears cyan (or turquoise). The superposition of the two filters returns one of the fundamental colors. The superposition of all 3 filters produces black: that is, the absence of light. In figure 3a and 3b shows two examples of additive synthesis and subtractive synthesis in borderline

cases which serve to obtain respectively the white light and the complete absence of light that is black.
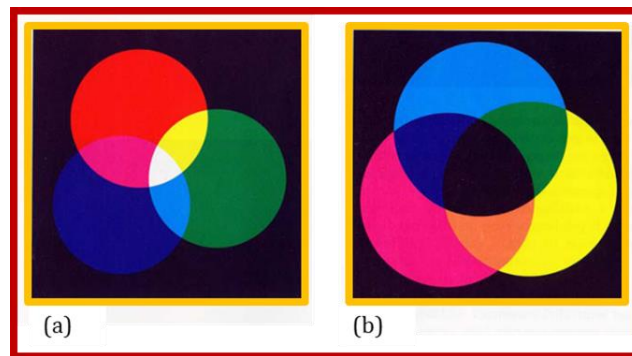

Figure 3. (a) additive synthesis to obtain white light with three primary colors; (b) subtractive synthesis for obtaining black with three primary filters.

The color that we perceive of a surface or of an object is the result of how to combine the light, usually white with a spectral composition similar to that of the Sun that lights our subject (illuminant) with the nature of the surface itself which could reflect differently the various wavelengths contained in the light illuminating it. Therefore, the true color of a surface is described by a curve, the spectral reflectance, which indicates the amount of light that is reflected, for each wavelength. The reflectance does not depend on the used light. A red surface does not reflect wavelengths corresponding to blue and green, but only those in the red. A bright red surface will reflect much the wavelengths of red in major measure, meanwhile, a dark red surface will reflect the red component in minor measure.

In order for a surface to appear illuminated, or is visible, it is necessary that the spectrum of the light source and the spectral reflectance of the surface have a spectrum portion in common (Figure 4).
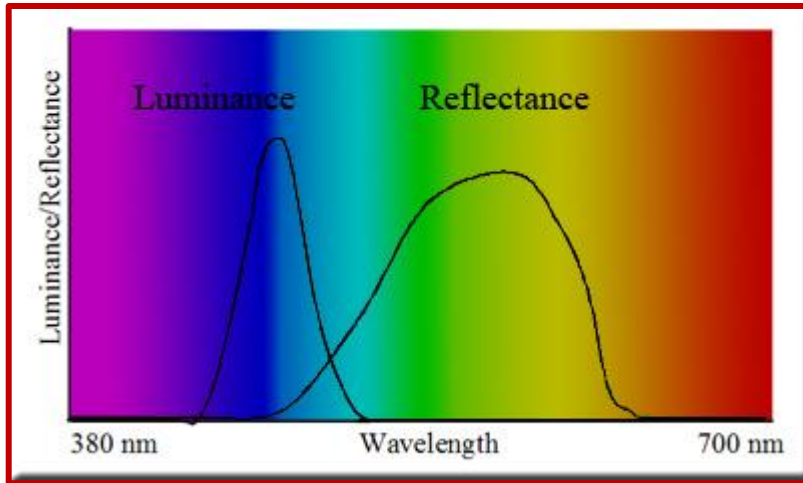
Figure 4. Overlay between spectrum of light and spectral reflectance

4.2 Hue, Saturation and Value space.

The literature describes different methods developed to quantify the color changes of a surface. These methods find their foundations on the color spaces that differently describe this property. The color spaces can be classified into four categories, connected by different types of mathematical transformations: linear light tristimulus, this color space was created by the International Commission on Illumination (CIE) (CIE XYZ, and CIE RGB), xy chromaticity (CIE xyY), perceptually uniform, and hue oriented (HLS, HSV)[1]. Scanners, digital cameras, and thus also smartphone's camera use red, green, blue (RGB) color space. It describes an image as an additive representation of all colors consisting of different combinations of red, green and blue [2]. When using the HSV color space to analyze a digital image, the pixels are described by hue, saturation and value coordinates, which are derived mathematically from the values red, green and blue. Hue is a numerical representation of color. Saturation determines the degree to which a single channel dominates; it is the purity or shade of a color. Value represents color brightness or lightness. The mathematical formulas that allow us to convert the RGB into HSV values are as follows:

$$H = \cos^{-1}\left\{\frac{\frac{1}{2}[(R-G)+(R-B)]}{\sqrt{(R-G)^2+(R-B)(G-B)}}\right\} \qquad \text{(eq. 1)}$$

$$S = 1 - \frac{3}{R+G+B}[\min(R,G,B)] \qquad \text{(eq. 2)}$$

$$V = \frac{1}{3}(R + G + B) \qquad \text{(eq. 3)}$$

R, G, and B values are the red, green, and blue color intensities, respectively and min represents the minimum values of R, G, and B. Hue is effected by wavelength of light, and by the Bezold-Brucke effect and the Abney effect. In accordance with the Bezold-Brucke effect, the hue values responds to changing the brightness or intensity of light. As brightness increases reds and yellows will become more orange and yellow [3]. The Abney effect is the notion that as white light is added (desaturation) hue will change; blue will appear more purple and orange will appear more red [3]. The main difference between the HSV and RGB color space is that HSV takes into account intensity of the image whereas, RGB does not, unable to differentiate small qualitative variations of the image that the RGB system alone is not able to do. Furthermore HSV space uses the intensity of the red, green, and blue color values [4]. The three dimensional representation of HSV is a hexacone (Figure 5).
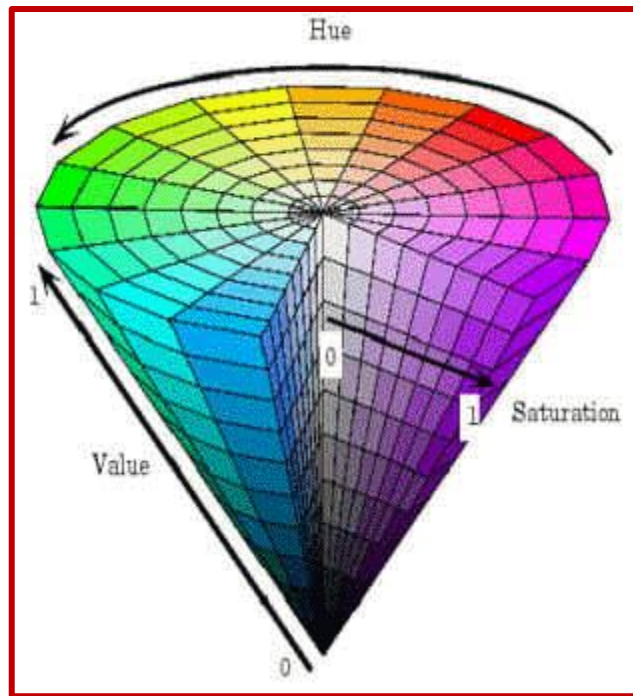
Figure 5. The HSV hexacone[5]

In reference system of HSV hexacone, Value can take all the values that are located along the central vertical axis. Hue is represented by the angle built around the central axis and can range from zero to 2π. Finally, Saturation represents the purity of the color, and can assume all values from the origin of zero central axis to the outer surface of hexacone. The Hue represents the color, Saturation represents the shade of color, and Value is essentially the gray scales of color. The value axis moves from black to white and gets there via various shades of grey. If saturation is decreased while hue and value remain fixed the resultant color will be a shade of grey. The shade of grey is dependent upon value. If saturation is at or near zero all of the pixels will appear the same, but as it is at or near one the pixels are separate and can be perceived as color.

4.3 Smartphone's technology and human eye capabilities comparison

The concept of light immediately involves the concept of the mechanism of the vision and perception around us. The light is a particular magnitude as its definition and its extent depend not only from objective physical quantity, but also from human visual system. For light means electromagnetic radiation, in particular those included in the range between 380 nm and 760 nm, can stimulate the human eye retina, producing the visual sensation.
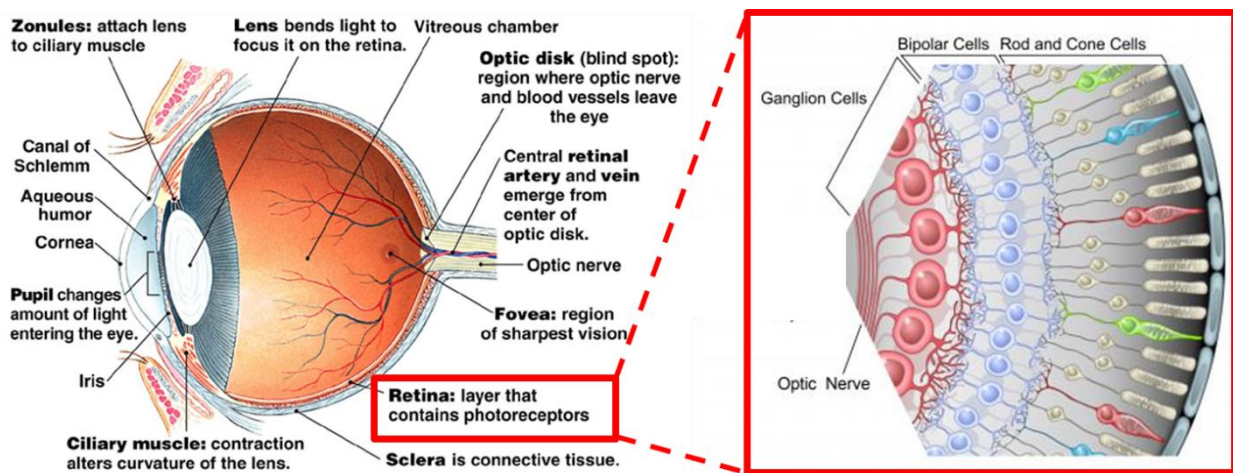

Figure 6. Human eye structure.

The structure of the human eye can be viewed in Figure 6. Light enters the eye via the cornea and is focused by the lens [6]. The eye's light sensor is a layered structure about 0.5 millimeters (mm) thick. This sensor covers about 70 percent of the surface of the eyeball. The human eye photoreceptors are of two types: rods and cones. These photoreceptors are constituted by two segments: one inner and one outer. The photons are detected by the outer segment portion of retina. While cones in the eye are sensitive to color, rods are sensitive to light intensity. Moreover, the human eye is sensitive to a minimum of about five photons. Each rod is sensitive to one photon and rods are excited by a photon when it induces an electrochemical reaction. Optimally, the human eye can resolve an image if the angle between two

points is equal to or greater than a critical value. The human eye can be compared to a smartphone's camera, as the camera was originally designed to mimic the eye.

Human Eye	Iphone 5 Camera
Iris (2-8 mm, dependant on intensity of light)	Aperture (f/2.4)
Cornea and Lens	Lens
Retina	CCD (digital images, film)

Table 1: Human eye to Iphone5 comparison

Table 1 presents this comparison, "image" quality of the eye will improve with a smaller iris aperture size, because as aperture size decreases it uses the optimal part of the lens and increases the depth of field [7].

4.4 Colorimetric Smartphone Applications

An assay is an analytical method in medicinal and biological research which measures the presence and the amount of an entity of interest. Among the most common assays in the clinical chemistry, there are methods relying on color change. These tests can be performated in liquid phase, by means of cuvettes or plates (Figure 7), or can be of paper-based. Measuring the change in color or absorbance, it is unable to quantify the analyte concentration.
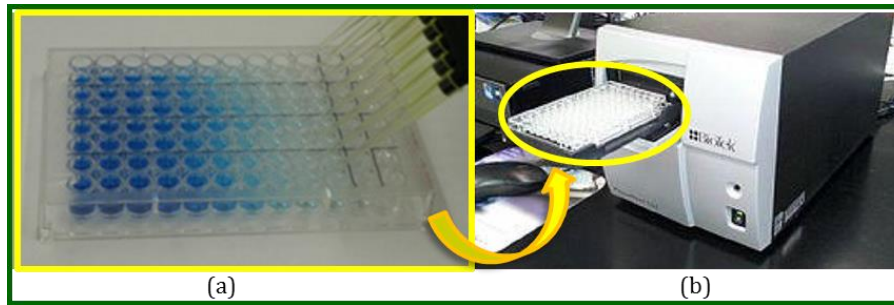
Figure 7. (a) Example of an assay plate with color changes; (b) A microplate reader with a 96 well microtiter plate

The results of this kind of assays are often determined by measuring the change in a color and its intensity. Thanks to their computation and optical capabilities, cellphones are unable to easily measure the color intensities. The use of a smartphone as a mobile plate reader, it could make the analysis easier and more economical, and provide the opportunity to conduct assays out of a standard laboratory. Even if portability plays a big advantage, on the other hand the accuracy and precision of the measurements made with a portable plate reader depend on the difficulty of controlling variables such as ambient light, color calibration and distance from point of measurement, which are constant for a commercial plate reader. For this reason, to better control all these variables and use smartphone as portable plate reader, it is necessary to fabricate an external housing or attachment for the phone.

4.4.1 Smartphone Camera Technology

The majority of smartphones use complimentary metal-oxide semiconductor (CMOS) cameras[8]. The CMOS camera circuit consists of an array of identical photo sensors in a grid. The light that reaches the photo sensor is converted to a digital signal by the camera circuit [9]. A colour filter array (CFA) with a Bayer pattern is placed over the photo sensor array (Figure 8) [10]. The CFA consists of a grid of red, green and blue filters and each photo sensor only

measures one colour band of the spectrum. Images are therefore the sum of distinct signals according to a RGB pattern. The intensity of the captured colours is directly proportional to the number of photons for each colour band [11]. The pattern is designed to capture an image similar to what a human eye would see. Moreover, smartphone cameras integrate a range of automated functions, such as Auto White Balance (AWB), which is designed to provide good color reproduction by adjusting the detected RGB signals at different ratios.
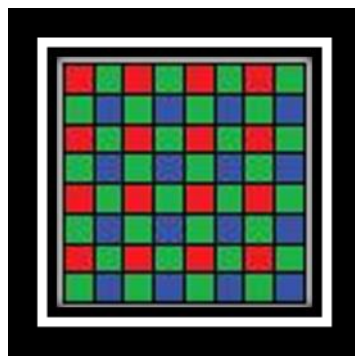

Figure 8. Bayer RGB filter pattern

Smartphone CMOS cameras have Bayer colour filters over the photo sensor array to respond to the red, green and blue bands of the visual spectrum, based on the trichromatic theory, from which arises the RGB space. As the camera has physical filters on which color determination depends, the RGB color space is defined as being device dependent [12]. The RGB color space is device dependent and vary from device to device due to different camera capabilities. Thus the measured colors are often converted to other color systems.

4.4.2 Smartphone Liquid Assay Readers

A typical smartphone-based liquid assay reader setup has been described by the research group of Vashist. It consists of a dark hood, a smartphone as an image reader and a tablet as a backlight illumination source as depicted in Figure 9 [13]. The dark hood has the task of isolating the detection zone from ambient light to avoid interference during image processing. The integration of a tablet backlight as light source ensures an equal illumination for the colorimetric test. Thanks to the image processing algorithm, that analyses the colour channel of the RGB spectrum depending on the type of assay, it is possible to determine the concentration by referencing that colour's calibration curve.

Figure 9. Box setup for point of care mobile plate reader.

A key feature of standard plate readers is that they are able to measure specific wavelengths of light, in the same manner as spectrophotometers, which allows the measurement of absorbance assays. The CMOS camera in mobile phones makes use of three built-in physical filters to separate the incoming light into the three color bands in the RGB space. Each filter has its own specific wavelength and thus the CMOS camera as a whole cannot be programmed to measure a single particular frequency such as traditional plate readers.

4.4.3 Smartphone Paper Assay Readers

Paper based assays easier than liquid assays. However, the results are less accurate and the responses of these devices are more suitable to qualitative or semi-quantitative analysis. as they place a greater emphasis on producing qualitative or quantitative results with lower Also in this case, color determination is subject to development of a calibration curve.

L. Shen et al. propose using a colour reference chart with 12 colours of known colour intensities (Figure 10) [14].First a photo of the reference card is taken in the same conditions as the measurement to follow. The colours are transformed into the C.I.E. colour space to avoid potential interference with built-in camera functions. B. Chang developed a similar paper colorimetric system (Figure 10) except using an image processing algorithm based on the HSV colour system - to avoid the inaccuracies in the standard RGB colour space [15]. The purpose of the reference chart is to reduce the effect of any lighting conditions which may impact the accuracy of colour determination.
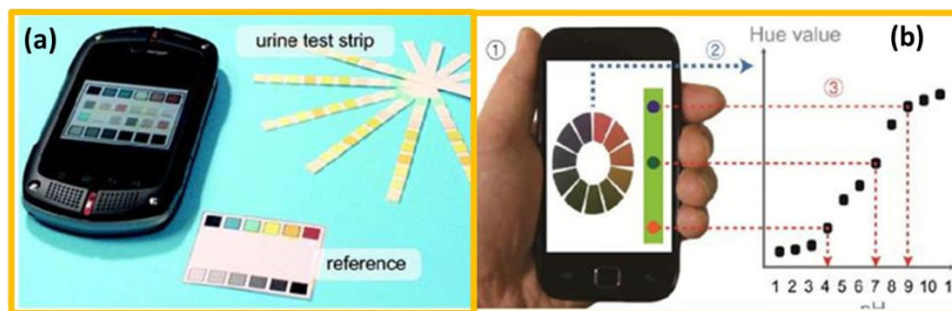

Figure 10. Examples of colour reference chart paper

4.4.4 Limits of color-change smartphone based devices

Although smartphones have integrated color-balancing functions, the smartphone camera is optimized for photography in high ambient light, and it is hard to control lighting conditions during imaging. This is especially true outside of controlled environments, such laboratories, and so it is difficult to

perform accurate quantitative measurements. Furthermore, analyzing the images is not always easy, especially when there are small changes in color. In these cases, it is not always possible to use the RGB space. Instead, an alternative, such as HSV or CIE, must be used. For all these reasons, when developing colorimetric tests to integrate with smartphones, phone-specific external housing units are often required. These units eliminate the variation in lighting conditions and camera positioning. Dedicated software and additional components, such as batteries, LED arrays (for reflection and transmission), and lenses, can further overcome these limitations and allow accurate measurements to be performed.

4.5 TMB Dye

The 3,3 ', 5,5'-tetramethylbenzidine (or TMB) is an aromatic amine. Its empirical formula is $C_{16}H_{20}N_2$ and the molecular weight of compound is 240,35 g/mol. Its solubility in aqueous solutions is 8,2 mg/L at 25°C. At room temperature is presented as a whitish solid faint smell, while colors of a delicate blue-green in a slightly acidic solution. TMB is degraded by sunlight or UV. It is slightly soluble in water, while it has a high solubility in ethanol. The TMB is a derivative of benzidine and is one of the most widespread chromogenic non-carcinogenic for analyzes based on the peroxidase detection [16], is used in immunohistochemistry and as the peroxidase detector in the ELISA technique [Sigma Aldrich Catalog Entry for 3,3′,5,5′-Tetramethylbenzidine].
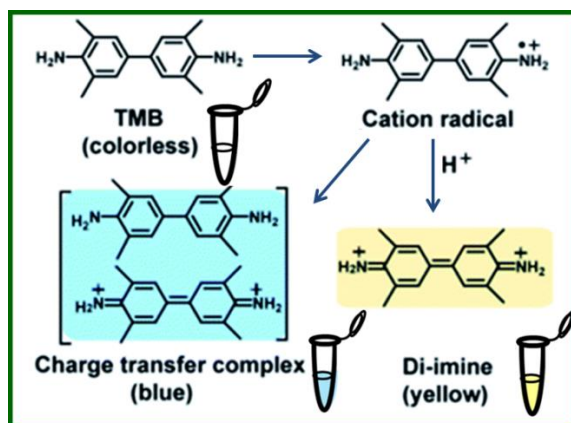
Figure 11. Oxidation scheme of TMB

TMB can act as electronic donor for the reduction of hydrogen peroxide to water by means of an enzyme having peroxidase as the peroxidase action, for example the widespread horseradish peroxidase or, with slower mechanism, cytochrome c. Under the enzymatic action, the TMB assumes a blue coloring with absorption peaks at wavelengths of 370 nm and 650 nm. In slightly acidic solution (pH 4-7) the colorless TMB can undergo two successive single-electron oxidation processes. The first stage leads to the formation of the intermediate radical product, which subsequently forms a complex at charge transfer with another radical of TMB, absorbing at 370 and 650 nm [17]. In a second stage is slowly form a chinodiimmina, which is the fully oxidized final product, absorbing at 450 nm [18][19][20].
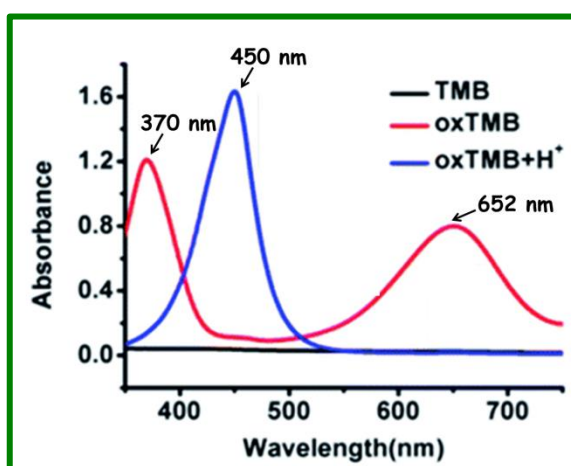

Figure 12. Changes in the spectrum of TMB due to oxidation enzyme

4.6 Properties of paper: an ideal material for bioassay.

Paper-based sensors are a new alternative technology for fabricating simple, low-cost, portable and disposable analytical devices for many application areas including clinical diagnosis, food quality control and environmental monitoring. The unique properties of paper which allow passive liquid transport and compatibility with chemicals/biochemicals are the main advantages of using paper as a sensing platform.

Paper has drawn much interest as a potential material for sensors and devices in analytical and clinical chemistry because of its versatility, high abundance and low cost [21][22][23]. These analytical devices can be integrated in a manner that is flexible, portable, disposable and easy to operate.

There are several techniques and processes involving chemical modification and/or physical deposition that could be used to tune the properties of the paper such that it becomes available for further modification or direct usage in a range of applications [24]. A lot of techniques focused on confining the liquid to a specific region on the paper have been reported in the literature: they include photolithography [25], analogue plotting [26], inkjet printing [27] and etching [28], plasma treatment [29], paper cutting [30], wax printing [31], flexography printing [32], screen printing [33], and laser treatment [34].

Colorimetric detection is probably the most suitable option for this kind of device, since results can be read by the nacked eye without the use of additional equipment. Concerning surface properties, specifically wettability, paper presents an advantage over nitrocellulose, since it is hydrophilic in nature and does not require additional processing steps. In order to compare

the surface morphology of nitrocellulose and cellulose based paper, figure 13 shows their microstructures obtained by scanning electron microscopy.
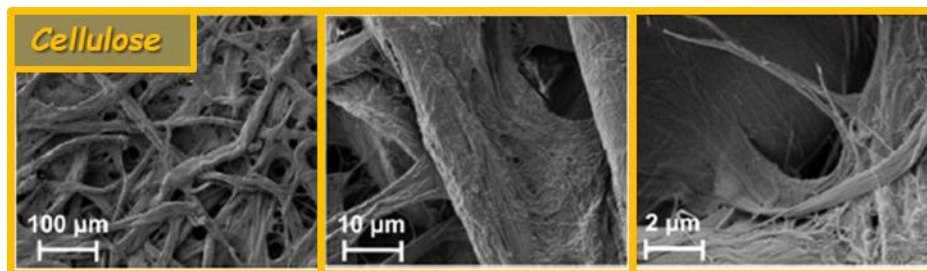

Figure 13. Scanning electron microscopy of chromatography paper Whatman no. 1

It is clear that besides having a completely different microstructure, chromatography paper Whatman no. 1 has a higher porosity (68%) with a corresponding higher pore diameter (100 μm) than nitrocellulose Whatman BA85 Protran (0,45 μm), to which corresponds a much lower contact angle, of 12°. Although nitrocellulose has been widely used for biological and clinical assays, it is not an ideal matrix for lateral flow devices. It does have certain amenable characteristics, such as high protein binding capacity and capillary flow properties, and it is available in a variety of products with varying wicking rates and surfactant contents. However, it is a highly flammable material, expensive when compared to paper, and presents low mechanical properties (brittle), which make it difficult to handle, and to pattern. Cellulose based paper does not have these disadvantages and has the ideal properties for the development of point of care colorimetric diagnostic platforms. So cellulose presents several advantages and has ideal properties for the development of point of care colorimetric diagnostic platforms.

Although there are several drawbacks associated with this technology, the most remarkable one is the heterogeneity of the color distribution in the detection zones. This issue, which can be attributed to the mobility of enzymes and reagents towards the edge of the detection zone when the

sample wicks up the hydrophilic channels, can result in increased variability and poor judgment of the final color by the user [35]. Several strategies can be adopted to overcome this problem, including controlling the volume of reactants and the sample's wicking velocity [36]. Among those directed to the immobilization of the enzymes via chemical modification to the cellulose [37] µPADs can also be modified using ceria nanoparticles [38], gold nanoparticles [39], silver nanoparticles,[40] and carbon nanotubes [41] to aid with the detection step. Although each of these strategies presents their own advantages, they are not widely applicable and require the implementation of specific processes. Aiming to address these shortcomings, the hypothesis of this project was that silica nanoparticles, trapped within the structure of the cellulose, could provide a simple and efficient way to immobilize the components of the analysis and therefore improve the overall performance of colorimetric detection on µPADs, since can provide a white background.

4.7 Cellulose chemical modification by Layer by layer.

Polyelectrolyte LbL deposition was introduced by Decher et al. in 1991. Thin multilayer films were assembled layer-wise onto a variety of surfaces by means of alternating deposition of polyanions and polycations [42]. The LbL-technique can be applied to solvent accessible surfaces of almost any kind and any shape, the more exotic ones being colloids, fruit, textiles, paper or, even biological cells. One of the key advantages of LbL-assembly is that LbL-films often display close to identical properties after deposition of the first few layers, even if films are deposited on very different surfaces. Most of the multilayer films have been fabricated using mainly electrostatic attraction as the driving force for multilayer build-up, this is by no means a prerequisite. There are many other interactions that have successfully been used for

multilayer deposition including: donor/acceptor interactions, hydrogen bridging, adsorption/drying cycles, covalent bonds, stereocomplex formation or specific recognition. The driving forces leading to PEM films is the electrostatic interaction between oppositely charged chains. Indeed there is not only an enthalpic contribution due to the interactions between point charges on the oppositely polyelectrolyte chains, but also an entropic contribution due to chain dehydration, conformational changes, and release of counter ions. Usually the balance between enthalpic and entropic contributions changes with the salt concentration of the solution and with temperature. Thanks to mechanical and porosity properties of this kind of films, enzymes can be encapsulated in such films and remain active for longer time durations than in solution.
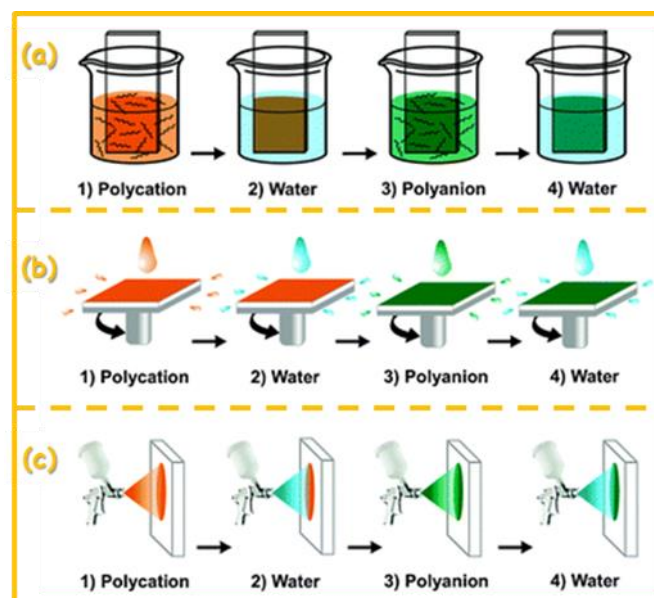

Figure 14. Schematic representation of the processes used to fabricate polyelectrolyte multilayer films by LbL assembly. (a) Dipping LbL assembly. (b) Spin-assisted LbL assembly. (c) Spray-assisted LbL assembly. Multilayer films are formed by repeating steps 1 to 4 in a cyclic fashion.

The methods to obtain Layer-by-Layer assemblies can be classified in three fabrication processes: Dipping LbL assembly, Spin-assisted LbL assembly and Spray-assisted LbL assembly. In the case of the conventional solution-dipping method, polyelectrolyte chains are allowed to diffuse toward the substrate

under the influence of the electrostatic interaction and then the adsorbed chains rearrange themselves on the surface. On the other hand, in the spin-coating process, the adsorption and rearrangement of adsorbed chains on the surface, and the elimination of weakly bound polymer chains from the substrate are almost simultaneously achieved at a high spinning speed for a short time. Spray-LbL, which consists of spraying the polyelectrolyte and rinse solutions directly onto a stationary vertical substrate. The convection of the spray droplets to the substrate surface created by the high pressure gas is the main driving force for Spray-LbL. As the droplets impact the surface, the polyelectrolyte chains must diffuse across a micron scale thin water film resulting from the drop impingement on the substrate, and onto the charged surface. The Spray-LbL method exposes the substrate to this atomized spray of polyelectrolyte solution for a short period of time, typically 3-10 seconds.

References

[1] Cantrell, K., Erenas, M. M., Orbe-Paya, I., Capitan-Vallvey, L. F.; (2010) Analytical Chemistry; 82: 531-542

[2] Kekre, H. B., Sonawane, K.; (2008) International Journal of Engineering Science and Technology; 4: 1233-1243.

[3] Erenas, M. M., Cantrell, K., Ballesta-Claver, J., Orbe-Paya, I., Capitan-Vallvey, L. F.; (2012) Sensors and Actuators B: Chemical; 147: 10-17.

[4] Kulp, T. D., Fuld, K.; (1995) Vision Research; 35: 2967-2983.

[5] Capel-Cuevas, S., Cuellar, M. P., Orbe-Paya, I., Pegalajar, M. C., Capitan-Vallvey, L. F.; (2010) Analytica Chimica Acta; 281: 71-81

[6] Davidovits, P.; (2008) *Physics in Biology and Medicine.* Elsevier Inc., San Diego. p. 214-237.

[7]Davidovits, P.; (2008) *Physics in Biology and Medicine.* Elsevier Inc., San Diego. 2008: p. 214-237.

[8] Reinhard, E., Khan, E.A., Akyz, A.O. and Johnson, G.M.; (2008). Color imaging: fundamentals and applications. AK Peters, Ltd.

[9]El Gamal, A. and Eltoukhy, H. (2005) CMOS image sensors. *Circuits and Devices Magazine, IEEE* 21, 6-20.

[10]Reinhard, E., Khan, E.A., Akyz, A.O. and Johnson, G.M.; (2008). Color imaging: fundamentals and applications. AK Peters, Ltd.

[11] Long, K.D., Yu, H. and Cunningham, B.T. (2014) *Biomedical optics express* 5: 3792-3806.

[12] Tkalcic, M. and Tasic, J.F. (2003) Colour spaces: perceptual, historical and applicational background. In *Eurocon,* Anonymous , 304-308.

[13]Vashist, S.K., Van Oordt, T., Schneider, E.M., Zengerle, R., Von Stetten, F. and Luong, J.H.T. (2015) *Biosensors and Bioelectronics* 67: 248-255.

[14]Shen, L.; Hagen, J.A.; and Papautisky, I.; (2012) *Lab on a Chip* 12, 4240-4243.

[15] Chang, B. (2012) *Bull. Korean Chem. Soc* 33: 549.

[16] Cattaneo M.V.; Luong J.H.; (1994) Analytical Biochemistry, 223(2): 313-320, DOI:10.1006/abio.1994.1590, ISSN 0003-2697.

[17] Yasuhito M., Yasuhide O., Tsuyoshi M., Koichi I.;(1997) J. Electroanal. Chem.; 436 (1-2): 203-212, DOI:10.1016/S0022-0728(97)00305-7, ISSN 0022-0728.

[18] Josephy P.D., Eling T., Mason R.P., (1982) J. Biol. Chem.; 257 (7): 3669 -3675.

[19] Yang T., Jiao K., Wang Z.J.;(2005) Chin. J.ournal of Appl. Chem.; 22 (4): 355-360

[20] Jiao K., Yang T., Wang Z.J.; (2004) Chin. Chem. Lett.;16 (5): 655-658.

[21] Martinez, A.W.; Phillips, S.T.; Whitesides, G.M.; Carrilho, E.; (2010) *Anal. Chem. 82:* 3–10

[22] Zhao, W.A.; van den Berg, A.; (2008) *Lab Chip*; *8:* 1988–1991

[23]Hossain, S.M.Z.; Luckham, R.E.; Smith, A.M.; Lebert, J.M.; Davies, L.M.; Pelton, R.H.; Filipe, C.D.M.; Brennan, J.D. (2009) *Anal. Chem.*, *81*: 5474–5483.

[24] Li, X.; Ballerini, D.R.; Shen, W.; (2012) *Biomicrofluidics 6:* 011301.

[25] Martinez, A.W.; Phillips, S.T.; Butte, M.J.; Whitesides, G.M.; (2007) *Angew. Chem. Int. Ed.* **;***46*: 1318–1320

[26]Bruzewicz, D.A.; Reches, M.; Whitesides, G.M.;(2008) *Anal. Chem.; 80*: 3387–3392

[27] Khan, M.S.; Fon, D.; Li, X.; Tian, J.F.; Forsythe, J.; Garnier, G.; Shen, W.; (2010) *Colloid Surf. B: Biointerfaces; 75*: 441–447

[28] Abe, K.; Suzuki, K.; Citterio, D.; (2008) *Anal. Chem.; 80*: 6928–6934

[29] Li, X.; Tian, J.F.; Shen, W.; (2010) *Cellulose*;*17*: 649–659

[30] Fenton, E.M.; Mascarenas, M.R.; Lopez, G.P.; Sibbett, S.S.; (2009) *ACS Appl. Mater. Inter.*; *1*: 124–129

[31]Lu, Y.; Shi, W.W.; Jiang, L.; Qin, J.H.; Lin, B.C.; (2009) *Electrophoresis; 30*: 1497–1500

[32] Olkkonen, J.; Lehtinen, K.; Erho, T.; (2010) *Anal. Chem.; 82*: 10246–10250

[33]Dungchai, W.; Chailapakul, O.; Henry, C.S.; (2011) *Analyst; 136*: 77–82

[34] Chitnis, G.; Ding, Z.W.; Chang, C.L.; Savran, C.A.; Ziaie, B. (2011) *Lab Chip; 11*: 1161–1165.

[35] Yetisen A.K.; Akram M.S. and Lowe C.R.; (2013) Lab Chip; 13: 2210–2251

[36] E. Evans E.; Gabriel E. F. M.; Coltro W. K. T. and Garcia C. D.; (2014) Analyst;139: 2127–2132

[37] D. M. Lewis and K. A. McLlroy; (1997) Rev. Prog. Color. Relat. Top.; 27: 5–17

[38] M. Ornatska, E. Sharpe, D. Andreescu and S. Andreescu; (2011) Anal. Chem.;83: 4273–4280

[39] S. Senkbeil, T. G. Jensen and J. P. Kutter, (2012) Lab Chip; 12: 4651–4656

[40] N. Ratnarathorn, O. Chailapakul, C. S. Henry and W. Dungchai;(2012) Talanta; 99: 552–557

[41] K. F. Lei, K.F. Lee and S.-I. Yang; (2012) Microelectron. Eng.; 100: 1-5

[42]G. Decher and J. D. Hong, (1991) Macromol. Chem. Macromol. Symp.; 46: 321–327

CHAPTER 5

SMARTPHONE EMBEDDED ENZYMATIC REFLECTANCE COLOR-BASED

BIOSENSOR FOR POINT-OF-NEED APPLICATION

5.1 Introduction and aim

The widespread availability, affordability, mobility and sophisticated technology of smartphones has enabled them to be used for much more than communication alone. The advance in camera technology has encouraged a range of applications. A lot of colorimetric apps are developed by which accurate colour measurement is possible and this enables a single mobile phone to become an accurate spectrophotometer, colorimeter and plate reader at a fraction of the cost of the traditional machines. Among all the available reporting systems, colorimetric detection is the most popular, simple and straightforward method for producing signals on paper-based biosensors, due to specific enzymatic or chemical interaction. To enable colorimetric diagnosis in multimedia devices, color must be expressed in numeric coordinates. An image of a diagnostic paper is analyzed digitally to yield a mathematical representation of color by incorporating color models, such as RGB. The color primaries are changed as function of ambient illumination. The advantage of using HSV coordinates over RGB for smartphone-based colorimetric imaging has been demonstrated in several publications [1][2][3]. The most remarkable drawback, associated with this technology, is the use of multiple reagents and the heterogeneity of the color distribution in the detection zones. This issue can be attributed to the mobility of enzymes and reagents towards the edge of detection zone when the sample is applied onto paper surface. With paper functionalization and chemical modification of cellulose [4][5][6], using layer by layer assembly technique, it is possible to realize a reagentless portable device and improve the heterogeneity of the color distribution [7]. We provide a simple and efficient way to immobilize all the components of the analysis on paper using the formation of a bilayer films of polyelectrolytes systems PAH-PSS coating the assay support. As application, we realized a portable smartphone-based

device to quantify lactate concentration in saliva.

5.2 Materials and methods

5.2.1 Chemicals

Peroxidase (type VI-A from horseradish, 1080 U mg^{-1} protein), L-lactate oxidase (from Pediococcus sp., 50 U mg^{-1} protein), L-lactate sodium salt, 3,3',5,5'-tetramethylbenzidine (TMB), Poly(allylamine hydrochloride), Poly(styrenesulfonate), L-histidine monohydrochloride mono-hydrate, mucin (type II from porcine stomach) and urea were supplied from Sigma Aldrich (St. Louis, MO). Sodium chloride, disodium hydrogen orthophosphate anhydrous, sodium dihydrogen orthophosphate monohydrate were supplied from Carlo Erba Reagents S.r.l. (Milano, Italy). Artificial saliva at pH 7.2 was prepared by dissolving 0.6 mg mL^{-1} Na$_2$HPO$_4$, 0.6 mg mL^{-1} anhydrous CaCl$_2$, 0.4 mg mL^{-1} KCl, 0.4 mg mL^{-1} NaCl, 4.0 mg mL^{-1} mucin and 4.0 mg mL^{-1} urea in deionised water according to Tlili et al. [8]. The colorimetric lactate enzymatic assay in the standard 96-well microtiter plate format (BioVision Incorporated L-Lactate colorimetric Assay Kit) was bought from BioVision Incorporated, Inc. U.S.A. and used according to the manufacturer's instructions.

## 5.2.2 3D printed analytical device fabrication
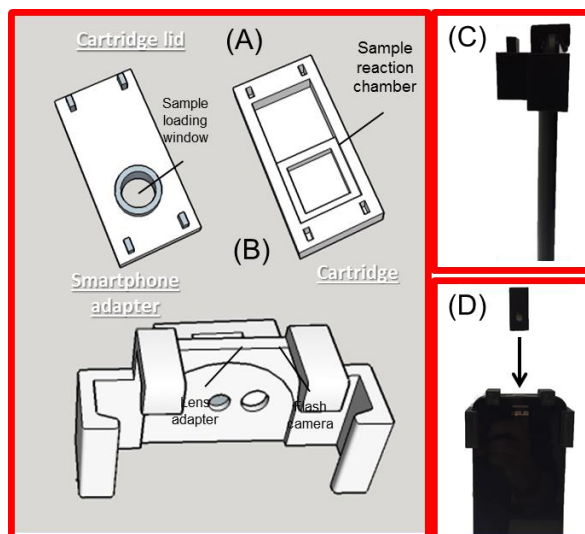
Figure 1. The 3D printed analytical device made of black ABS polymers consisting of three separate components: a disposable analytical cartridge, a mini dark box, and a smartphone adapter. (A) Cross-sections of the analytical cartridge and the cartridge lid and (B) the horizontal section of the analytical cartridge showing the internal chambers and fluidic connections. (C) Photo of the cartridge-lid assembly and of the mini dark box and smartphone adapter.

The analytical device (Figure 1) is made of black acrylonitrile-butadiene-styrene (ABS) polymers and was produced using a low-cost commercial 3D printer (Replicator 2X Desktop 3D Printer, MakerBot Industries, New York, NY). The device was designed using the open-source SckechUp software (Trimble Navigation). Files were exported as .stl les and MakerWare v.2.4 software, an algorithm that slices digital into thin layers for 3D printing, was used to define printing options and settings. The device consists of three separate components: (a) a disposable analytical cartridge, (b) a mini dark box, and (c) a smartphone adapter. The analytical cartridge (20 mm × 10 mm) contains one reaction chamber (diameter 4 mm, depth 3 mm) with small 1cm × 1cm paper support of the cellulose, onto which LOx, HRP and TMB are entrapped in bilayer film (PAH/PSS). The enzyme amounts immobilized on the disks were as follows: LOx 0.02 U (for saliva analysis), horseradish peroxidase 0.1 U. The mini dark box contains the analytical cartridge during

the measurement, ensuring its correct positioning and avoiding interference from ambient light. As source of light is used the flash built-in of smartphone. The smartphone adapter holds the mini dark box and can be snapped onto the smartphone to correctly position the dark box in relation to the smartphone embedded camera. The adapter includes a plano-convex plastic lens (diameter 6 mm, focus 12 mm), which focuses the image of the reaction chambers of the cartridge onto the smartphone camera and a flash diffuser to homogenize the light toward the detection area.

5.2.3 Assay procedure

Oral fluid is collected by a salivette. Then, a volume of 50 μl of sample is applied in reaction chamber of the cartridge. The cartridge is then inserted into the mini dark box camera, which is already snapped to the smartphone. The color change signal is measured by using the smartphone camera. Suitable smartphone photography apps are used to control the exposure time (which must be long enough to achieve the required detectability) and for image handling. For android-based smartphones, we used the Camera FV-5 (Android) Lite app to perform image acquisitions, after 60s from sample loading. Quantitative analysis of the images was performed using the open source so ware ImageJ v.1.46 (National Institutes of Health, Bethesda, MD). Regions of interest (ROIs) corresponding to the sample and control detection chambers, as well as a ROI of the same dimension in a dark area of each image for subtraction of the background signal, were selected. Color change on detection area were quantified as HUE value. GraphPad Prism v. 5.04 (GraphPad So ware, Inc., La Jolla, CA) was used to plot the HUE value as a

function of lactate concentration and for least-squares fitting of calibration curves.

5.3 Results and discussion

The aim of this work was to develop a reagentless portable lactate color change based biosensor for assessing L-lactate levels in oral fluid, based on the coupling of the enzymatic oxidation of lactate catalyzed by L-lactate oxidase with the TMB/H_2O_2/HRP colorimetric system. The novelty and the skills of this color-based biosensor are in no need of multiple reagents. All of components and reagents to perform the analysis are entrapped on assay support. The assay started when only sample is loaded on test PAD. We designed a simple device using disposable analytical cartridges to allow measurement of the color change of assay support relying on reflectance principle of light, produced by the enzyme reaction using a smartphone embedded camera. This device exploits the backside-illumination complementary metal-oxide semiconductor (BI-CMOS) sensors integrated into modern smartphones. These offer improved low-light performance and color and brightness control in comparison with conventional front-illuminated CMOS sensors. The device also takes advantage of low-cost 3D printing technologies, which allowed the rapid prototyping and production of device components.

5.3.1 Correlation between lactate levels and color-change based assay

In order to quantify the colorimetric reaction and to obtain the saliva lactate concentration value, we have developed a calibration curve linking lactate to HSV (Hue, Saturation, Lightness) hexaconical-coordinate representation of the RGB (Red, Green, Blue) color values at the center of the lactate test PAD.

Hue has a piecewise definition and in the region of interest of the lactate colorimetric reaction can be written as a function of the red (R), green (G), and blue (B) color values:

$$H = \cos^{-1}\left\{\frac{\frac{1}{2}[(R-G)+(R-B)]}{\sqrt{(R-G)^2+(R-B)(G-B)}}\right\} \qquad \text{(eq. 1)}$$

$$S = 1 - \frac{3}{R+G+B}[\min(R,G,B)] \qquad \text{(eq. 2)}$$

$$V = \frac{1}{3}(R + G + B) \qquad \text{(eq. 3)}$$

5.3.2 Flash Diffuser (Homogeneity of light)

The flash diffuser consists of a 5 mm thick membrane of polydimethylsiloxane (PDMS). The purpose of the flash diffuser is to reduce variations in the reading for different lighting conditions. It allows light from smartphone's flash to diffuse and illuminate the back of the test strip uniformly. In addition, the case is 3D printed using black ABS polymer material in order to isolate the test strip from variable external light. The case is designed in a way that minimizes the effect of external lighting. It has been seen that at low analyte concentrations, a light diffuser is needed so that the color change can be quantifiable. When no diffuser is used, the strip appears as white with either 100% or 0% saturation levels [9].


(a)   (b)
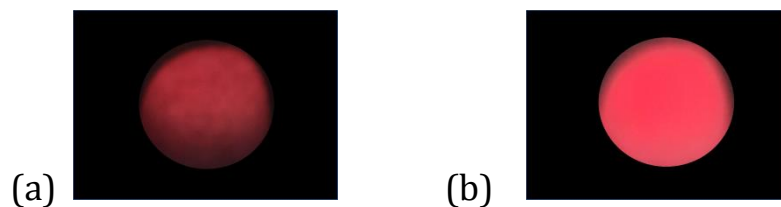
Figure 2. The figure illustrates the design of the case around the camera and flash that allows for uniform lighting of the test pad (with flash diffuser(a); without flash diffuser(b)).

By guiding the flash light through the PDMS diffuser on the pad, we avoid the need to build in a lighting element, such as a LED, that would make the system bulkier and require power input. The pad is imaged at a distance of 1,5 cm from the smartphone camera and the whole optical piece has a depth of 6 mm.

The wide range of variations across different devices and of test strip illumination present significant challenges to accurate colorimetric quantification. Other investigators have addressed this problem by calibrating for ambient light conditions through conversion to color spaces which are less sensitive to changes in brightness. This approach still requires uniform external illumination, and false colorimetric readings can be made if the phone is not placed at the proper distance from the test strip. Our device is isolated from ambient light with the hardware accessory and diffuses light from the smartphone camera flash for reproducible and uniform illumination, improving measurement accuracy and minimizing the potential for user error.

The accessory is designed in such a way as to illuminate the cellulose pad to ensure better uniformity of lighting on the circular detection area of the test strip. In order to improve the sensitivity of the system to variations in the color of the μPAD and to reduce the effect of μPAD misalignment into the device, we have incorporated a light diffuser over the flash (Figure 2).

5.3.3 Paper functionalization

The main disadvantage with this kind of paper test is the use of multiple reagents and the heterogeneity of the color distribution in the detection zones.

This problem can be attributed to the mobility of enzymes and reagents towards the edge of detection zone when the sample is applied onto paper surface. Cellulose functionalization with a nanomaterial, allows to realize a reagentless portable device and to improve the heterogeneity of the color distribution. We provide a simple and efficient way to immobilize all the components of the analysis on paper using the formation of a bilayer films of polyelectrolytes systems PAH-PSS coating the assay support (Figure 3).


(a)   (b)
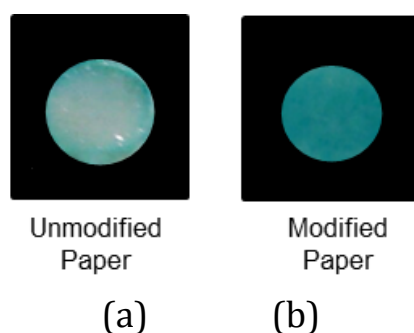
Figure 3. Images of mPAD unmodified (a) and modified (b) with polyelectrolites bilayer films.

Thanks to this functionalization, we obtain that the assay support is composed of a cellulose paper (1×1 cm) onto which enzymes (HRP and LOx) and a chromogenic substrate, 3,3',5,5'-tetramethylbenzydine (TMB), are entrapped using a bilayer component polymer coating of poly(styrene sulfonate) (PSS) and poly(allylamine hydrochloride) (PAH). The causes of omogeneity distribution of color on paper surface, reached with this method can be attributed to following reasons: the PAH/PSS films retarde the realease of TMB through the polyelectrolyte bilayer shells avoiding an

hetereougeneus diffusion through the paper, homogeneus loading of enzymes in polymer multilayer coating and the negative PSS layer reduces the mobility of charged intermediates of oxidated TMB.

Polyelectrolyte films were built by dipping the cellulose support in polycation (PAH) and polyanion (PSS) solutions, respectively. Dipping in PSS (1mg/ml), containing TMB (2 mM) and PAH (1mg/ml), containing enzymes solutions were performed. All reagents are prepared in PBS 0,1M, pH7,5. After each poly-ion adsorption, the paper membrane was rinsed three times in PBS 0,1 M, pH 7,5 (Figure 4).
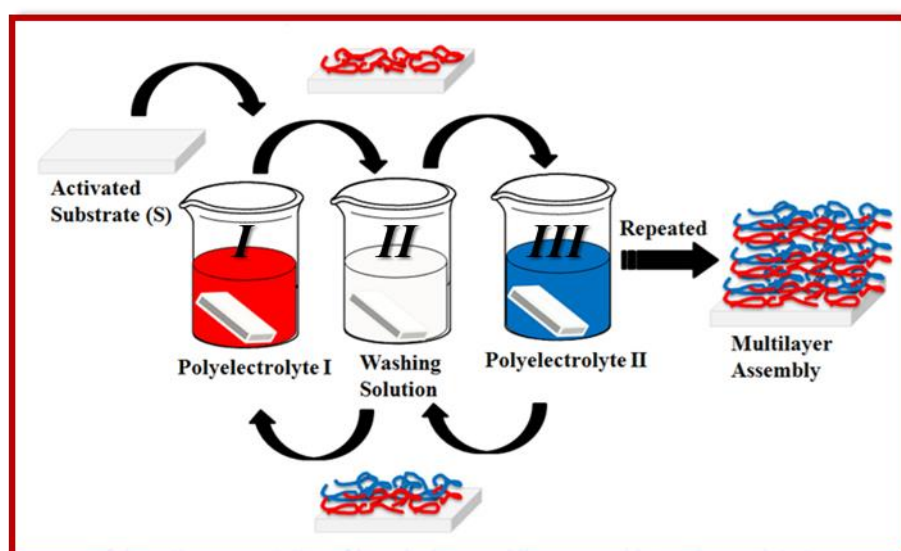

Figure 4. LbL protocol: dipping in 1. polyanion solution, 2. rinsing solution, 3. polycation solution, 4. rinsing solution.

Deposition speed is dependent on physical parameters (pH, ionic force, temperature) but also on the chemical nature of the components. In our conditions, the adsorption should be complete and homogeneous after a few minutes. The dipping time was fixed to 30 minutes to ensure complete layer deposition.

5.3.4 Calibration curve

The relationship between HUE value and lactate concentration for our PAD test was established using artificial oral fluid and TMB-HRP colorimetric systems for 5 points of calibration (Figure 5). The color change from the last reaction is then imaged inside the smartphone accessory by the smartphone camera. Limits of detection (LOD) of 0.6 mmol L^{-1} (corresponding to 5.4 mg dL^{-1}) of lactate were obtained in oral fluid.
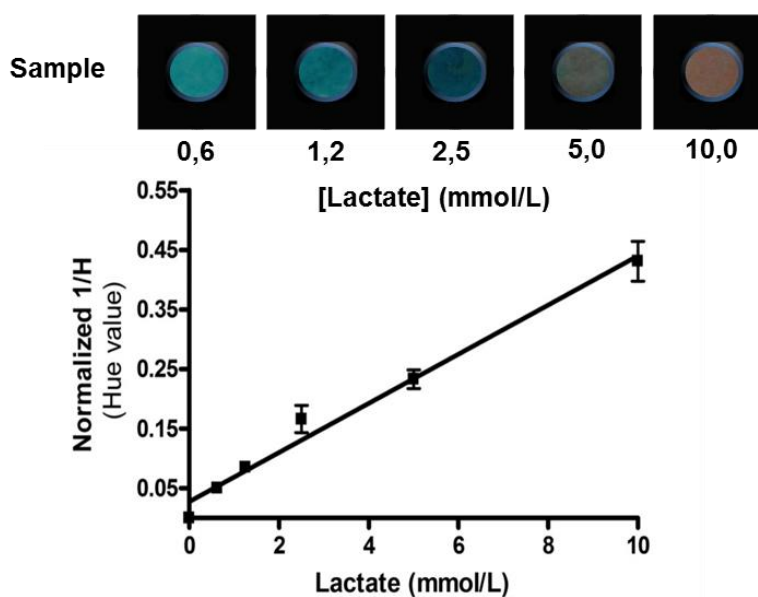

Figure 5. Lactate calibration curves obtained in artificial oral fluid. Hue values were normalized to the H value obtained for the blank sample of the same cartridge. Data points represent the mean ± SD of three replicates

5.3.5 Matrix effect

To perform a reliable measurement of lactate in real samples, the possible interference of oral fluid matrix on color-change result was evaluated. To study the matrix effect, we developed the analytical method and the calibration curve in artificial oral fluid.

5.3.6 Image Processing

To acquire the result image of colorimetric analysis of the lactate enzymatic reaction, has been used smartphone app dedicated to photo acquisition Camera FV-5 Lite. When the user takes a picture by the app, an image of the colorimetric color changes is acquired through the smartphone camera. Quantitative analysis of the images was performed using the open source so ware ImageJ v.1.46 (National Institutes of Health, Bethesda, MD). First, a 960 px by 960 px calibration area is selected at the center of the image. The average RGB value is computed and converted to HSV. This average HSV value is then compared to a reference value and a background shift is computed. The whole image is then subjected to this background shift. After the background shift, a 960 px by 960 px area in the middle of the detection circle is then selected and the same computation as before is done to obtain the average HSV value of the test area. In order to decrease fluctuations due to lightning conditions, the strip is imaged 3 times and the average hue value over those 3 images is taken. GraphPad Prism v. 5.04 (GraphPad So ware, Inc., La Jolla, CA) was used to plot the hue signal as a function of lactate concentration.

5.3.7 Accuracy and reproducibility (Time acquisition)

A critical issue to consider for point-of-care testing is the accuracy of the measurement. Once the user applies a drop of saliva (a volume of 50 microliters of sample) on the reaction area on the support of cellulose, it takes some time for the colorimetric change to occur. Enzymatic chemical reactions and the colorimetric change occurs gradually. If the PAD is imaged before the reaction has terminated then we will get a misleadingly low value for the saliva lactate level. In order to determine the approximate time

required for the reaction to occur we have monitored the color change for an oral fluid sample with an actual concentration of 2 mM. As can be seen in Figure 6, it takes about 60s for the colorimetric change to stabilize. It is therefore important to consider a time frame for imaging the test PAD. In addition averaging several acquired images during that time frame can helped further improve the accuracy.
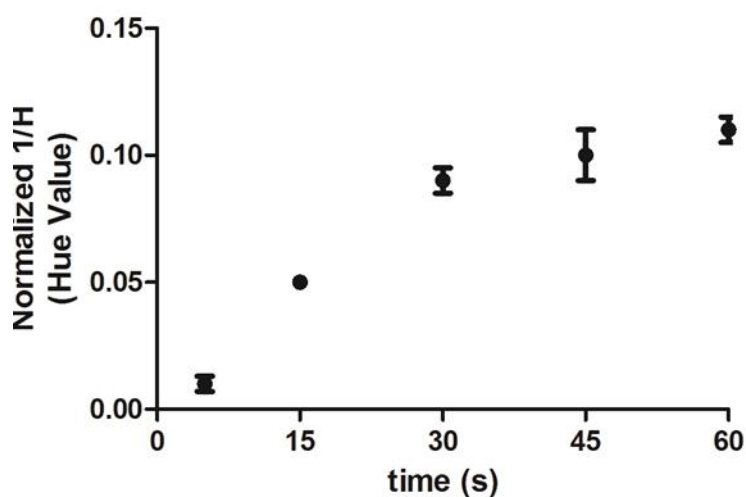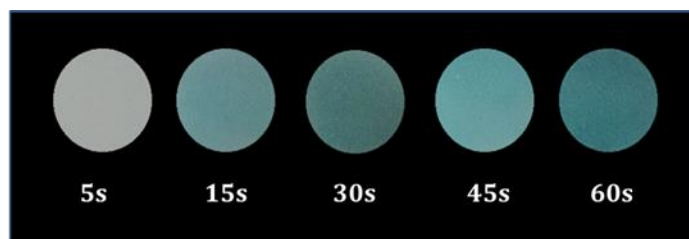

Figure 6. Different color images of lactate (2 mM) in time

5.3.8 Assay validation

To validate the assay, oral fluid samples were analyzed in parallel with the smartphone-based lactate biosensor and with a commercial colorimetric

lactate enzymatic assay in the standard 96-well microtiter plate format (BioVision Incorporated L-Lactate colorimetric Assay Kit). Reaction time is 30 min. at room temperature, and wavelength to read microplate is 570 nm. Figure 7 compares the concentrations measured in oral fluid and sweat samples, which indicated a good correlation between the effective concentration of lactate in the samples and the results obtained with the smartphone-based lactate biosensor.
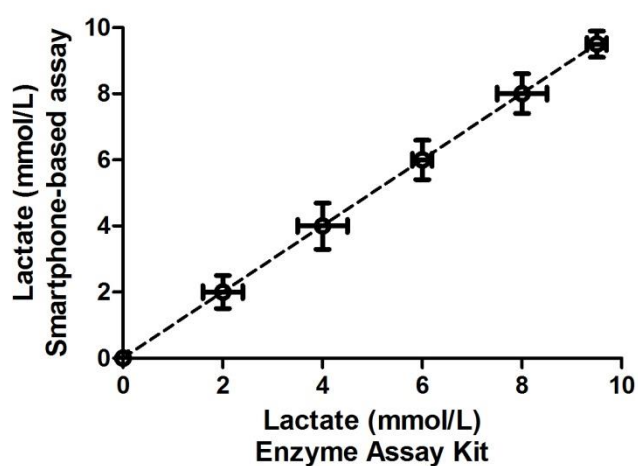

Figure 7. Comparison of the lactate concentrations measured in (A) oral fluid and (B) sweat samples using the smartphone-based lactate biosensor and a BioVision Incorporated L-Lactate colorimetric Assay Kit performed in the standard 96-well microtiter plate format. Each data represents the mean × SD of three replicates.

5.3.8 Application

To demonstrate the applicability of the smartphone-based biosensor for monitoring lactate levels during physical exercise, we measured the lactate in oral fluid during the running track performed by a volunteer. Figure 8 shows the saliva lactate pro le measured in the volunteer and obtained by collecting.
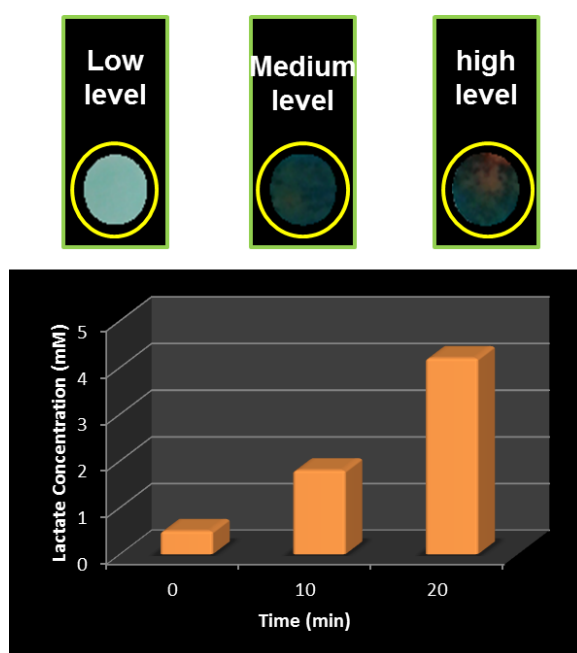

Figure 8. Images of lactate levels in saliva monitored by smartphone-based biosensor during the running track performed by a volunteer.

5.4 Conclusions

SmartAssay could be considered as the forerunner of the integration colorimetric detection on smartphones for point-of-care and point-of need analysis. Although less sensitive than techniques that exploit chemiluminescence as a detection principle, this method based on the color variation is a simple and rapid assay. It also allows us to monitor the variation of analyte in time. Moreover, the choise of cellulose as support for bioassay

presents several advantages and has ideal properties for the development of point of care colorimetric diagnostic platforms. In literature are present a lot of examples of using cellulose to develop paper-based analytical biosensor [10][11][12][13][14][15][16][17][18]. Chemical modification of cellulose by layer-by-layer (LbL) deposition of complementary polymers allows to realize a reagentless portable device and to improve the heterogeneity of the color distribution. The extreme simplicity of the device widens it applicability and makes it suitable for the detection of many analytes of clinical interest, for instance H_2O_2 producing oxidases such as those specific for glucose and ethanol.

References

[1] Oncescu V., O'Dell D. and Erickson D.; (2013) Lab Chip; 13: 3232-3238

[2]Chang B.Y.; (2012) Bull. Korean Chem. Soc.; 33: 549-552;

[3]Contrell K., Erenas M.M., De Orbe-Paya I. and Capitàn-Vallvey L.F.; (2010) Anal. Chem.; 82: 531-542

[4]Decher, G.; (1996) Layered nanoarchitectures via directed assembly of anionic and cationic molecules, in Templating, Self-Assembly and Self-Organization (eds J.-P. Sauvage and M.W. Hosseini), Pergamon Press, Oxford, pp. 507–528.

[5] Decher, G. and Hong, J.-D.; (1991) Makromol. Chem., Macromol. Symp., 46: 321–327.

[6] Izquierdo, A., Ono, S.S., Voegel, J.C.,Schaaf, P., and Decher, G.; (2005) Langmuir; 21: 7558–7567.

[7] Evans, E., Gabriel, E. F. M., Benavidez, T. E., Coltro, W. K. T., & Garcia, C. D.; (2014) *Analyst*, *139*(21): 5560-5567.

[8] C. Tlili, L.N. Cella, V.N. Myung, V. Shetty, Mulchandani; (2010) Analyst; 135: 2637–2642

[9] Oncescu, V., Mancuso, M., & Erickson, D. (2014). Lab on a Chip, 14(4), 759-763.

[10] Martinez, A.W.; Phillips, S.T.; Whitesides, G.M.; Carrilho, E.; (2010) Anal. Chem.; 82: 3–10.

[11] Yu, J.H.; Ge, L.; Huang, J.D.; Wang, S.M.; Ge, S.G.; (2011) Lab Chip; 11: 1286–1291.

[12] Fenton, E.M.; Mascarenas, M.R.; Lopez, G.P.; Sibbett, S.S.; (2009) ACS Appl. Mater. Inter.; 1: 124–129.

[13] Carvalhal, R.F.; Kfouri, M.S.; Piazetta, M.H.D.; Gobbi, A.L.; Kubota, L.T.; (2010) Anal. Chem.; 82: 1162–1165.

[14] Martinez, A.W.; Phillips, S.T.; Carrilho, E.; Thomas, S.W.; Sindi, H.; Whitesides, G.M.; (2008) Anal. Chem.; 80: 3699–3707.

[15] Apilux, A.; Dungchai, W.; Siangproh, W.; Praphairaksit, N.; Henry, C.S.; Chailapakul, O.; (2010) Anal. Chem.; 82: 1727–1732.

[16] Ellerbee, A.K.; Phillips, S.T.; Siegel, A.C.; Mirica, K.A.; Martinez, A.W.; Striehl, P.; Jain, N.; Prentiss, M.; Whitesides, G.M.; (2009) Anal. Chem.; 81: 8447–8452.

[17] Luckham, R.E.; Brennan, J.D.; (2010) Analyst; 135: 2028–2035.

[18] Bracher, P.J.; Gupta, M.; Whitesides, G.M.; (2010) Soft Matter; 6: 4303–4309.